Screening of Biochemical and Molecular Mechanisms of Secondary Injury and Repair in the Brain after Experimental Blast-Induced Traumatic Brain Injury in Rats

Patrick M. Kochanek,[1,2] C. Edward Dixon,[1,3] David K. Shellington,[8] Samuel S. Shin,[1,3] Hülya Bayır,[1,2,6,7] Edwin K. Jackson,[5] Valerian E. Kagan,[6,7] Hong Q. Yan,[1,3] Peter V. Swauger,[9] Steven A. Parks,[9] David V. Ritzel,[11] Richard Bauman,[10] Robert S.B. Clark,[1,2] Robert H. Garman,[4] Faris Bandak,[12, 13] Geoffrey Ling,[12] and Larry W. Jenkins[1,3]

[1]Safar Center for Resuscitation Research, [2]Departments of Critical Care Medicine, [3]Neurological Surgery, [4]Pathology, [5]Med-Pharmacology [6]Environmental and Occupational Health, and [7]Pittsburgh Center for Free Radical and Antioxidant Health, University of Pittsburgh School of Medicine, [8]Department of Pediatrics, University of California, San Diego; [9]ORA Inc., Fredericksburg, VA; [10]Walter Reed Army Institute of Research, Silver Spring, MD; [11]Dyn-FX Consulting Ltd, Amherstburg, ON; [12]Department of Neurology, F. Edward Hébert School of Medicine, Uniformed Services University of the Health Sciences, Bethesda, MD; [12]Integrated Services Group, Inc., Potomac, MD

Running Head: Screening molecular mechanisms after blast TBI in rats

Corresponding Author:

Patrick M Kochanek, MD, MCCM
Professor and Vice Chairman
Department of Critical Care Medicine
Professor of Anesthesiology, Pediatrics and Clinical and Translational Science
University of Pittsburgh School of Medicine
Safar Center for Resuscitation Research
3434 Fifth Avenue
Pittsburgh, PA 15260
Tel: (412) 383-1900
Fax: (412) 624-0943
Email: kochanekpm@ccm.upmc.edu

Report Documentation Page

Form Approved
OMB No. 0704-0188

1. REPORT DATE	2. REPORT TYPE	3. DATES COVERED
2013		**00-00-2013 to 00-00-2013**

4. TITLE AND SUBTITLE	5a. CONTRACT NUMBER
Screening of Biochemical and Molecular Mechanisms of Secondary Injury and Repair in the Brain after Experimental Blast-Induced Traumatic Brain Injury in Rats	5b. GRANT NUMBER
	5c. PROGRAM ELEMENT NUMBER
6. AUTHOR(S)	5d. PROJECT NUMBER
	5e. TASK NUMBER
	5f. WORK UNIT NUMBER
7. PERFORMING ORGANIZATION NAME(S) AND ADDRESS(ES) **Uniformed Services University of the Health,Sciences,Bethesda,MD,20814**	8. PERFORMING ORGANIZATION REPORT NUMBER
9. SPONSORING/MONITORING AGENCY NAME(S) AND ADDRESS(ES)	10. SPONSOR/MONITOR'S ACRONYM(S)
	11. SPONSOR/MONITOR'S REPORT NUMBER(S)

12. DISTRIBUTION/AVAILABILITY STATEMENT
Approved for public release; distribution unlimited

13. SUPPLEMENTARY NOTES
Journal of Neurotrauma, Preprint, March 17, 2013

14. ABSTRACT

15. SUBJECT TERMS

16. SECURITY CLASSIFICATION OF:			17. LIMITATION OF ABSTRACT	18. NUMBER OF PAGES	19a. NAME OF RESPONSIBLE PERSON
a. REPORT **unclassified**	b. ABSTRACT **unclassified**	c. THIS PAGE **unclassified**	**Same as Report (SAR)**	**65**	

Patrick M. Kochanek, MD, MCCM
Professor and Vice Chairman
Department of Critical Care Medicine
Professor of Anesthesiology, Pediatrics and Clinical and Translational Science
University of Pittsburgh School of Medicine
Safar Center for Resuscitation Research
3434 Fifth Avenue
Pittsburgh, PA 15260
Tel: (412) 383-1900
Fax: (412) 624-0943
Email: kochanekpm@ccm.upmc.edu

C. Edward Dixon, PhD
Department of Neurological Surgery
University of Pittsburgh School of Medicine
Safar Center for Resuscitation Research
3434 Fifth Avenue
Pittsburgh, PA 15260
Tel: (412) 383-2188
Fax: (412) 624-0943
Email: dixoce@upmc.edu

David K. Shellington, MD
Associate Physician Dipl.
Department of Pediatrics
University of California at San Diego
9500 Gilman Drive 0984
La Jolla, CA 92093-0984
Tel: (757) 270-8880
Email: dshellington@ucsd.edu

Samuel S. Shin, PhD
Department of Neurological Surgery
University of Pittsburgh School of Medicine
Safar Center for Resuscitation Research
3434 Fifth Avenue
Pittsburgh, PA 15260
Tel: (412) 383-2188
Fax: (412) 624-0943
Email: shinss@upmc.edu

Hülya Bayır, MD
Assistant Professor
Critical Care Medicine and Department of Environmental and Occupational Health
Children's Hospital of Pittsburgh of UPMC
Department of Critical Care Medicine
University of Pittsburgh School of Medicine
4401 Penn Avenue, Suite Floor 5
Pittsburgh, PA 15224
Tel: (412) 692-5164
Fax: (412) 692-6076

Email: bayihx@ccm.upmc.edu

Edwin K. Jackson, PhD
Center for Clinical Pharmacology
University of Pittsburgh School of Medicine
Cellomics Building, Suite 450
100 Technology Drive
Pittsburgh, PA 15217
Tel: (412) 648-1505
Email: edj+@pitt.edu

Valerian E. Kagan, PhD, DSci
Center for Free Radical and Antioxidant Health
Department of Environmental and Occupational Health
University of Pittsburgh
Bridgeside Point
100 Technology Drive, Suite 350
Pittsburgh, PA
Tel: (412) 624-9479
Fax: (412) 624-9361
E-mail: kagan@pitt.edu

Hong Qu Yan, MD, PhD
Research Assistant Professor
Department of Neurological Surgery
University of Pittsburgh School of Medicine
Safar Center for Resuscitation Research
3434 Fifth Avenue
Pittsburgh, PA 15260
Tel: (4120 383-2188
Fax: (412) 624-0943
Email: hyan+@pitt.edu

Mr. Peter V. Swauger
Associate Research Scientist, ORA Inc.
Fredericksburg, VA
Tel: (540) 809-2077
Fax: (540) 368-1190
Email: pswauger@ora-inc.com

Mr. Steven A. Parks
President, ORA Inc.
71 Commerce Parkway
Fredericksburg, VA 22406
Tel: (540) 809-2077
Fax: (540) 368-1190
Email: sparks@ora-inc.com

David V. Ritzel, PhD
Senior Analyst

Dyn-FX Consulting Ltd.
Amherstburg, ON
Tel: (519) 817-7489
Fax:(519) 736-5065
Email: dritz@dyn-fx.com

Richard A. Bauman, PhD
Walter Reed Army Institute of Research
Division of Military Casualty Research
Department of Polytrauma & Resuscitation
502 Robert Grant Avenue
Silver Spring, MD 20910-7500
Tel: (301) 319-9059
Fax: (301) 319-9706
Email: Richard.bauman@amedd.army.mil

Robert S.B. Clark, MD
Chief, Pediatric Critical Care Medicine
Children's Hospital of Pittsburgh of UPMC
Associate Professor, Critical Care Medicine and Pediatrics
Department of Critical Care Medicine
University of Pittsburgh School of Medicine
4401 Penn Avenue, Suite Floor 5
Pittsburgh, PA 15224
Tel: (412) 692-5164
Fax: (412) 692-6076
Email: clarkrs@ccm.upmc.edu

Robert H. Garman, DVM, DACVP
Department of Pathology
University of Pittsburgh School of Medicine
P.O. Box 68
Murrysville, PA 15668-0068
Tel: (724) 733-5154
Fax: (724) 733-3032
Email: vetpathol@cs.com

Faris A. Bandak, PhD
Professor
Department of Neurology, A1036
F. Edward Hébert School of Medicine
Uniformed Services University of the Health Sciences
4301 Jones Bridge
Bethesda, Maryland 20814
Tel: (301) 299-7357
Email: fbandak@usuhs.mil

Geoffrey S. Ling, MD, PhD
Department of Neurology
F. Edward Hébert School of Medicine

Uniformed Services University of the Health Sciences
Bethesda, MD 20814
Email: Geoffrey.Ling@darpa.mil

Larry W. Jenkins, PhD
Department of Neurological Surgery
University of Pittsburgh School of Medicine
Safar Center for Resuscitation Research
3434 Fifth Avenue
Pittsburgh, PA 15260
Tel: (412) 383-2188
Fax: (412) 624-0943
Email: ljenkins@pitt.edu

Abstract

Explosive Blast-induced traumatic brain injury (TBI) is the signature insult in modern combat casualty care and has been linked to posttraumatic stress disorder, memory loss, and chronic traumatic encephalopathy. We reported on blast induced mild TBI (mTBI) characterized by fiber-tract degeneration and axonal injury revealed by cupric silver staining in adult male rats after head only exposure to 35 PSI in a helium-driven shock tube with head restraint. We now explore pathways of secondary injury and repair using biochemical/molecular strategies. Injury produced ~25% mortality from apnea. Shams received identical anesthesia exposure. Rats were sacrificed at 2h or 24h and brain sampled in hippocampus and pre-frontal cortex. Hippocampal samples were used to assess gene array (RatRef-12 Expression BeadChip) and oxidative stress (ascorbate, glutathione [GSH], low molecular weight thiols [LMWT], protein thiols, and 4-hydroxynonenal [HNE]). Cortical samples were used to assess neuroinflammation (cytokines, chemokines, and growth factors; Luminex) and purines (ATP, ADP, adenosine, inosine, 2'-AMP, and 5'-AMP). Gene array revealed marked increases in astrocyte and neuroinflammatory markers at 24h (GFAP, Vimentin, complement component 1) with expression patterns bioinformatically consistent with those seen in Alzheimer's disease and long-term potentiation. Ascorbate, LMWT, and protein thiols were reduced at 2 and 24h; by 24h HNE was increased. At 2h, multiple cytokines and chemokines (IL-1α, IL-6, IL-10, MIP-1α), were increased; by 24h only MIP-1α remained elevated. ATP was not depleted and adenosine correlated with 2'- not 5'-cAMP. Our data reveal 1) gene array alterations similar to disorders of memory processing and a marked astrocyte response, 2) oxidative stress, 2) neuroinflammation with a sustained chemokine response, and 3) adenosine production despite lack of energy failure—possibly resulting from metabolism of 2'-3'-cAMP. A robust biochemical/molecular response occurs after blast induced mTBI with the body protected from blast and the head constrained to limit motion.

Key Words: Axonal Injury, Improvised Explosive Device, Combat Casualty Care, Cytokine, Chemokine, Gene Array, Multiplex, antioxidant, ascorbate, glutathione, lipid peroxidation, purine, adenosine, cyclic-AMP, ATP, post traumatic stress disorder

Introduction

Explosive blast induced traumatic brain injury (TBI) has taken on enormous importance in U.S. combat casualty care. Information on the pathobiology and neuropathology of blast TBI in humans—particularly cases of mild injury uncomplicated by prior history of head impact — is limited. Mac Donald et al[1] using diffusion tensor imaging (DTI) revealed axonal injury in deep white matter in soldiers with mild TBI within three months of exposure improvised explosive device blast with another blast related event such as a fall or a motor vehicle crash. Goldstein et al[2] reported on neuropathology of three military veterans exposed to blast TBI and a fourth who experienced multiple non-blast concussions. Perivascular Tau was seen along with axonal degeneration. Based on parallel studies of blast (shock tube) exposure in rats, Goldstein and coworkers suggested a limited role for direct head blast or thoracic-mediated mechanisms, but implicated resulting rotational head acceleration in producing the injury. Other studies in blast TBI models have reported axonal injury using a blast loading ranging from shock tubes to explosive blast in several species; including studies with and without head motion constraint.[3-11]

Studies in experimental models have, however, provided few clues as to underlying pathomechanisms mediating secondary damage and/or dysfunction after blast TBI. In addition, many soldiers with posttraumatic stress disorder (PTSD) have no abnormalities on conventional brain imaging[1,12] despite explosive blast exposure, and it has been suggested that in some cases, pathological processes below the level of neuronal death or axonal injury–such as alterations in brain activation or cell signaling could be important.[13-15] An approach to screen mechanisms in a blast TBI model at the threshold of detectible neuropathology could provide useful insight into therapeutic targets. Clues as to possible secondary injury mechanisms after experimental blast TBI were first provided by Cernak et al[10] who reported a role for oxidative stress and neuroinflammation[16], but studies are limited.

The Defense Advanced Research Projects Agency of the U.S. Department of Defense established the *Preventing Violent Explosive Neurologic Trauma* (PREVENT) program, to link experts in blast physics and injury biomechanics, experimental and clinical TBI, neuropathology, and pharmacology to study explosive blast TBI across species and models, link explosive physics with biology, explore the biophysics and pathomechanisms of injury, and evaluate potential therapies and diagnostics. A component of the program includes studies using a rat shock tube model. In a report on the neuropathology in that model, Garman et al[11] showed that a head only simulated free field exposure with a peak pressure of ~35 psi and a positive phase duration of ~4 milliseconds, producing ~25% mortality, in rats with total body shielding and head constraint, resulted in axonal injury in deep white matter structures including both cerebellum and brainstem, consistent with the clinical report of Mac Donald et al[1] and also with a more recent report showing that in uncomplicated blast injury in soldiers, DTI changes are seen in the deep white matter of the cerebellum (personal communication, from the senior author, Dr. David Brody). Consistent fiber tract injury in the hippocampus bilaterally but rare neuronal death was observed. It was clear that the lesions reported by Garman et al[11] were relatively mild, given that they were detectible only with highly sensitive cupric silver staining; other signatures of injury were limited.

A key question that remains is whether or not an uncomplicated blast exposure at mild injury levels produces substantive biochemical and/or molecular changes and if these are unique. One might posit that the secondary injury cascade in blast TBI resembles that seen in any type of TBI. However, reports from blast TBI victims suggest that there are unique findings across the injury spectrum, such as a strong link to PTSD after mild blast TBI, and rapid and malignant brain swelling and vasospasm after severe blast TBI.[17,18] Thus, an approach to screening secondary injury and neuroprotectant cascades after a blast exposure could help in determining if there are unique biochemical and/or molecular signatures. Assessment of these

mechanisms at an injury level near the threshold of neuropathological damage could also provide insight as to whether primary uncomplicated blast exposure could produce biochemical and/or molecular alterations that might underlie important sequelae such as PTSD or memory loss in the absence of neuronal death. We thus undertook a broad screening approach to secondary injury mechanisms in blast TBI in injured rat brain tissue that included 1) assessment of a gene array, 2) assessment of cytokines, chemokines, and growth factors using a Multiplex-based array, 3) assessment of markers of oxidative stress, and 4) assessment of levels of ATP, purine metabolites and the endogenous neuroprotectant adenosine in our established blast TBI model in rats. We screened all of these mechanisms in the same rats to address whether or not they occurred concomitantly. We hypothesized that mild to moderate uncomplicated primary blast exposure limited to brain can induce a robust secondary injury response in rat brain.

Methods

Blast TBI model in rats

Male Sprague Dawley rats (n = 17, Charles River Laboratories) were studied, 11 exposed to blast and 6 shams. The rats were between 350g and 425g in weight at the time of injury. Details of the insult were previously reported.[11] Briefly, using an IACUC-approved protocol, the bodies of isoflurane-anesthetized rats (2% isoflurane in air) were shielded in a steel wedge that was supported by a rod positioned 7 ft (2130 mm) from the end of a 14 ft (4270 mm) helium-driven shock tube. A fully-formed decay profile developed in the waveform at the test station (due to the reflected rarefaction from the driver), and there were no artifacts from either open-end rarefaction or contact surface in the blast simulation. Surface-flush PCB gauges were used for the shock measurements. A diaphragm of 3x0.004" Mylar layers was used because it produced a faster and more complete rupture than a single 0.012" Mylar sheet; a sharp shock front had fully formed by the test station. The driver gas was helium charged into an initial volume of ambient air; this helium/air mix ensures a negligible density discontinuity at the 'contact surface' interface between the expanding driver gases and shocked air although in fact that interface did not affect the test station. Due to the inefficiencies of plastic diaphragm rupture, the driver was pressurized to well above the value expected from theory. This shock tube generated a well-defined, uniform, and highly reproducible shockwave with a peak pressure of ~35 PSI and a positive phase-duration of ~4 milliseconds as previously reported.[11] A steel wedge in the shock tube ("Mach Stem Device") was designed to protect the thorax and abdomen of the rat, as well as to enhance the shock wave intensity. Details of this device along with the time pressure profile that is produced were recently published.[11] The design ensured that the triple point of the resultant Mach stem passed well above the head and thereby imparted a uniform shock-wave exposure. The apex of the wedge pointed toward the incident shock front and, at the apex, the incident shock front skimmed off the surface of the wedge

producing an amplified reflected wave - a Mach stem - that impinged on the left side of the rat's head. The rat's head was located 29.5 inches (75 mm) along the ramp face from the leading edge - with the head being 7 feet (2130 mm) from the shock tube muzzle and 14 feet (4270 mm) from the Mylar diaphragm.

In order to isolate the effects of the blast shock and assure that any ensuing brain damage would have been the result of the shock only without significant effects from impact or acceleration, the rats' heads were constrained against a compliant leather 'sling' fitted between two short posts to ensure minimal whole head motion. In our prior report, the blast exposure in the shock tube produced an injury with ~25% mortality from apnea.[11]

Surviving rats were allowed to recover from anesthesia and randomized to follow up for either 2 h or 24 h. Shams, subjected to an identical anesthetic exposure as injured, were allowed to recover in an identical manner and also followed for either 2 h or 24 h. Injuries were performed at ORA laboratories.

Overall approach to tissue sampling

The analyses and respective sites at which they were carried out included 1) Gene array analysis at the University of Pittsburgh Genetics Core, 2) Multiplex for cytokines, chemokines, and growth factors at the University of Pittsburgh Multiplex Core Facility/Pittsburgh Cancer Institute, 3) biochemical markers of oxidative stress and oxidative injury at the University of Pittsburgh Center for Free Radical and Antioxidant Health, and 4) analysis of levels of ATP, purine metabolites and adenosine at the University of Pittsburgh Department of Pharmacology and Chemical Biology. Tissue processing requirements for the various assays to be performed were different and highly specific for each laboratory. In addition, concerns over potential

freeze-thaw artifacts related to partitioning samples, and the need to supply each laboratory with adequate tissue sample volume were also important considerations. Thus, we chose to provide each laboratory consistent samples by apportioning a specific brain structure to each mechanism/laboratory, namely, hippocampus ipsilateral to blast exposure for Gene Array, cortex ipsilateral to blast exposure for Multiplex analysis, hippocampus contralateral to blast exposure for markers of oxidative stress and cortex contralateral to blast exposure for ATP, purines, and adenosine. The rationale for this approach is also supported by our prior description of the neuropathology in this model which revealed similar degrees of axonal injury (the principle neuropathological finding) on the right and left sides of the brain.[11] A diagram of the specific brain tissue distribution plan is shown in Figure 1.

Brains were removed in whole at 2 h and 24 h after injury, rapidly dissected to define and isolate hippocampus and frontal-parietal cortex both ipsilateral and contralateral to blast exposure. Samples were flash frozen in liquid nitrogen for subsequent analysis. For these exploratory studies, rats were injured until a total of n = 3 per group and n = 4 per group survived until the pre-defined sacrificed time point of 2 h or 24 h post-injury, respectively. Shams (n = 3 per group) were also generated for each of the 2 h and 24 h time points.

Gene array

Total RNA was isolated using the Ambion RNAqueous®-Micro RNA isolation kit (Applied Biosystems, Austin, TX). RNA Amplification and conjugation were performed using the BD Biosciences Super SMART RNA amplification and labeling system (Clontech Laboratories, Inc. Mountain View, CA), per manufacturer instructions. Biotinilated cRNA was hybridized to an Illumina RatRef-12 Expression BeadChip for genome-wide expression analysis (Illumina, Inc., San Diego, CA). The BeadChip was processed and scanned per manufacturer instructions. Based on an efficiency analysis, performed to determine the analysis method and

normalization/feature selection combination leading to the most internally consistent gene set,[19] data was normalized with $\log_2$ and z-transformation, and the J5 test was used to identify differentially expressed genes.[20] A pathway level impact analysis was implemented, which was designed to provide both statistical and biological significance in indicating the pathways affected by observed gene expression changes.[21] The results are summarized as impact scores and p-values. The Gene Expression Pattern Grids (GEPD)[20] were also used to prioritize the genes considered to be differentially expressed in most samples for each group-wise comparison (Figure 2). The GEPD allows the direct visualization of the status of the genes in each sample in the microarray data. In this study, we focused on GEPD groups which included genes whose expression distributions tend to be unambiguously non-overlapping.

Multiplex assessment of cytokines, chemokines, and growth factors

The frozen frontal-parietal cortical tissue samples were weighed and placed in 5x volume of PBS. Brain tissue was homogenized in PBS, sonicated, and centrifuged for 30 min at 14,000 x g for 30 min. Supernatant was collected and used for Multiplex analysis.

Multiplex cytokine assays (Invitrogen) were processed according to the manufacturer's instructions. Briefly, bead stock was vortexed, sonicated, and diluted from the 10x solution with Working Wash solution. The Standard and Sample wells in a 96-well plate were pre-wet with 200 µl of Working Wash solution. Solution was aspirated from the bottom of the wells via a prepared suction apparatus. Capture bead solution (25 µL) was added to each well. Incubation buffer was added to all wells as directed. Standards and samples were prepared in the first two columns as directed. The 96-well plate was placed in a dark room to avoid photo-bleaching of the beads and was incubated for 2 h on an orbital shaker.

After incubation, each well was aspirated and washed with 200 uL of Working Wash solution. Biotinylated Detector Antibody (100 µL) was added to each well and the plate was incubated for

an additional hour covered, on an orbital shaker. Streptavadin-RPE solution was diluted according to instructions and 100 µL was placed in each well. The plate was incubated for an additional 30 min. After an additional wash, the beads were resuspended in Working Wash Solution and read on a Luminex 200 instrument (Luminex, Austin, TX). The multiplex assay was performed at the University of Pittsburgh Cancer Institute Core Multiplex Facility. Protein concentration in each sample was determined via BCA assay (Thermo Fisher Scientific, Rockford, IL). Cytokine concentrations as determined by the multiplex assay were normalized to protein concentration and expressed as pg/mg protein. Twenty four proteins were included in the platform, namely, interleukin-1α (IL-1α), interleukin-1β (IL-1β), IL-2, IL-4, IL-5, IL-6, IL-9, IL-10, IL-12p70, IL-13, IL-17, IL-18, tumor necrosis factor alpha (TNFα), interferon gamma (IFNg), macrophage inflammatory protein-1α (MIP-1α), granulocyte colony stimulating factor (GCSF), granulocyte macrophage colony stimulating factor (GMCSF), growth related oncogene KC (GRO/KC), monocyte chemotactic protein-1 (MCP-1), eotaxin, Interferon gamma-induced protein 10 (IP-10), regulated upon activation, normal T-cell (RANTES), leptin, and vascular endothelial growth factor (VEGF).

Markers of oxidative stress and oxidative damage

Hippocampi were thawed on ice and homogenized using a Tissue Tearor (BioCold Scientific, Fenton, MO) in lysis buffer (tissue weight to volume ratio of 1:20) consisting of 30mM Tris HCl, 150mM NaCl, 1% Triton X-100 (Aldrich Chemicals, Milwaukee, WI) . Homogenates were centrifuged at 1000 × *g* for 10 min then divided into aliquots for analysis of protein, ascorbate, GSH, and 4-HNE. Metaphosphoric acid (MPA) was added to a final concentration of 5% (v/v) to the aliquot for ascorbate measurements and protease inhibitor cocktail (Sigma, St. Louis, MO) was added to the aliquot for 4-HNE assay, and all samples were stored at −80 °C until use.

Fluorescence assay of reduced glutathione (GSH), low molecular weight thiols (LMWT), and protein sulfhydryls. Protein concentration in the brain homogenates was determined using

working reagent (Bio-Rad Laboratories, Hercules, CA) with a Bovine Serum Albumin (BSA) standard (0.1mg/ml). A standard curve was established by addition of GSH (0.04-4mM) to 50 mM Na, Na-phosphate buffer, pH 7.4 containing 10 mM ThioGloTM-1 (Calbiochem, SanDiego, CA), a maleimid reagent that produces a highly fluorescent product upon its reaction with thiol groups.[21] GSH concentrations were determined by addition of GSH peroxidase and cumene hydro peroxide to the brain homogenates with ThioGloTM-1 working solution, and the resultant fluorescence response was subtracted from the LMWT measured by the fluorescence response of the same specimens with only the addition of ThioGloTM-1 (Calbiochem). Levels of total protein sulfhydryls were determined as fluorescence response after adding 4 mM SDS to each LMWT sample. A Fusion alpha plate reader (PerkinElmer/ Packard, Waltham, MA) was used to detect fluorescence at excitation and emission wavelengths of 388 and 500 nm, respectively. Samples were analyzed in triplicate.

Measurement of ascorbate levels. Hippocampal ascorbate levels were measured using a fluorescence assay as described previously.[23] Briefly, each sample was divided into two aliquots, each containing 0.1-0.6 mg/ml protein. To ensure the selectivity of the assay towards ascorbate one of the aliquots (50 µL) was treated with 1 U of ascorbate oxidase (AO) for 40 min at room temperature. Samples were transferred onto a 96-well plate along with ascorbate standards (0-1.5 nmols). After this, 130 µL AC-TEMPO stock aliquots (23.1 µM in phosphate buffer) were added immediately using a multi-channel pipette to each well and samples were incubated for 40 min at room temperature in the dark and analyzed using a Packard “Fusion α” multifunctional plate reader (PerkinElmer Life Sciences, Boston, MA). Fluorescence was measured using a 390±15 nm filter for excitation and 460±35 nm filter for emission. Fluorescence readings from the AO-treated samples were subtracted from non-treated and normalized to protein. Samples were analyzed in triplicate.

Detection of 4-Hydroxynonenal (HNE) protein Michael adducts. After separation by SDS–PAGE, proteins were transferred electrophoretically (190 V, 90 min) to nitrocellulose

membranes (Thermo Scientific Pierce, Rockford, IL), which were blocked (18 hr, 20ºC) with 5% nonfat milk in 0.01 mol/L phosphate-buffered saline (PBS), pH 7.4, 150 mmol/L NaCl, 0.05% Tween 20 (PBS-T). For detection of HNE protein Michael adducts, blots were incubated overnight at 4ºC with monoclonal mouse anti-HNE antibody (1: 2000 dilution in 1% BSA-T, R&D Systems, Minneapolis). For loading control, blots were incubated overnight at 4ºC with anti-actin antibody (1:10,000 dilution, Sigma, St. Louis, MO). After four 15 min washes in PBS-T, the immunocomplexed membranes were probed (1 hr, 20ºC) with an anti-rabbit (1: 5000 dilution, Jackson Immuno Research Laboratories, West Grove, PA) horseradish peroxidase conjugated secondary antibody. Probed membranes were washed (10 min, PBS-T) four times and immunoreactive proteins detected using Super Signal West Femto Kit (Thermo Scientific Pierce).

Measurement of Purines

Brain tissue samples were placed in liquid nitrogen, quick-smashed with a tissue clamp device that was kept in liquid nitrogen, and quick-smashed tissues were placed immediately in ice-cold perchloric acid containing 10-^{13}C-ATP (internal standard) or 1-propanol containing 10-^{13}C-adenosine (internal standard). Tubes containing the ice-cold stop solutions were pre-weighted so that the weight of brain tissue could be obtained by weighing the tubes after the brain tissue had been placed in the stop solution. After extraction of purines (1 h), samples were centrifuged and the supernatants were taken to dryness under vacuum and then reconstituted in distilled water. The brain samples placed in 1-propanol were analyzed for 3',5'-cAMP, 2',3'-cAMP, 5'-AMP, 3'-AMP, 2'-AMP, adenosine and inosine using our standard LC-MS/MS purine assay with selected reaction monitoring (SRM).[24] The brain samples placed in perchloric acid were analyzed for ATP and ADP also using LC-MS/MS but with modifications of our standard purine assay. For ATP and ADP, the HPLC reversed phase column was a Bonus-RP (1x 50 mm; 3.5 µm; Agilent technology), and the mobile phase consisted of two eluents. Eluent A was 5 mM

dimethylhexylamine at pH 7 and Eluent B was acetonitrile-water (70:30). The gradient (A/B) was: 0 to 1.2 min, 95%/5%; 5.5 min to 7.0 min 30%/70%; 8.0 to 12.0 min 95%/5%. The flow rate was 80 µl/min, and the column temperature was kept at 20° C. The SRM mass transitions monitored were: 506 → 408 for ATP with a collision energy of 18 volts; 516 → 418 for ^{13}C-ATP with a collision energy of 18 volts; and 426 → 328 for ADP with a collision energy of 18 volts. All results were normalized to tissue sample weight.

Data Analyses and Statistics

Data are presented as mean and SEM or as dot plots with corresponding median value as appropriate. Data analyses for the Gene array studies were previously outlined in the methods. For Multiplex, oxidative stress, and purine biomarker data, one way ANOVA was used followed by post-hoc comparison via Student-Newman-Keuls test or Kruskal-Wallis Test for data that were not normally distributed. Linear correlation was also used for the purine analyses.

Results

Blast TBI model in rats

It was necessary to generate 11 blast exposures to achieve the 8 surviving rats to the desired endpoints. Three of the 11 rats died of apnea immediately after the exposure, producing a ~27% mortality rate from apnea, which is nearly identical to the 25% mortality reported in our initial publication using this model at this injury level.[11] There was no delayed death.

Gene array

The microarray data showed a complex set of changes affecting multiple categories of cellular function after injury. Three comparisons were made: 1) Sham vs. Injured at 2 h after blast (Figure 2A and Table 1), 2) Sham vs. Injured at 24 h (Figure 2B and Table 2), and 3) Injured at 24 h vs. Injured at 2 h (Figure 2C). In these 3 comparisons, 21, 58, and 39 genes were differentially expressed, respectively.

Comparison of 2 h after blast TBI vs. sham

The first comparison showed that genes were mostly upregulated at 2 h after injury compared to shams, specifically, there were 18 upregulated genes and 3 downregulated genes (Figure 2A and Table 1). The most noticeable changes were increases in 7 ribosomal proteins (Rps10, Rpl29, Rpl35, Rpl41, Rps14, Rpl32, Rps26) in hippocampus. Three genes involved in mitochondrial respiration and electron transport (Cox7b, Ndufa11, Uqcrh) as well as hemoglobin alpha and beta chain genes (Hbb, Hba-a1) were also upregulated at 2 h.

In addition, pathway level impact analysis of the gene array data at 2 h after blast TBI was most consistent and most highly significantly associated with a ribosomal pattern likely reflecting the aforementioned rapid increases in gene expression of a variety of ribosomal, presumably for translation of key gene products in the early post TBI response. Three of the

four other patterns that showed statistically significant associations with blast TBI at 2 h included Parkinson's, Huntington's, and Alzheimer's disease, respectively suggesting similarities in the early blast TBI response to those seen in important neurodegenerative diseases that have been linked to TBI.[25]

Comparison of 24 h after blast TBI vs. sham

The second comparison showed that at 24 h after injury, hippocampal tissue had upregulation of 29 and downregulation of 29 genes indicating an important overall shift in gene expression pattern. Genes involved in differentiation, neurogenesis, and growth (Gap43, Prss11), as well as those involved in apoptosis and stress response (Hspb1, Mt1a, Anxa3, among others) were upregulated vs. sham. At 24 h, there was also increased expression of some genes involved in energy metabolism (Uqcrc2, Mdh1, Gpi, Aldoa) and transport function (solute carrier family 25, solute carrier family 3, mitochondrial membrane ATP synthase, Dncic1, Nsf). However, several other transport function-associated genes (Atp6v0c, Sv2b, Laptm4a, Atp2a2) were downregulated suggesting differential expression in this category. There was also a downregulation of calcium signaling associated genes at 24 h (Camk2n1, Camk2b, calreticulin) along with downregulation of several differentiation and growth related genes (Ndrg2, Rtn4, Cspg5).

Pathway level impact analysis of the gene array data at 24 h after blast TBI (Table 4) indicated that the blast TBI gene expression profile was significantly associated with 28 established pathways. Blast TBI gene expression was most significantly associated with two profiles importantly linked to learning and memory namely Alzheimer's disease and long term potentiation. The next two pathways that were most significantly associated with blast TBI with regard to gene expression profiles at 24 h included calcium signaling and VEGF signaling, and

Parkinson's disease was again significantly associated and in the top 10 most significant pathways at 24 h.

Comparison of 24 h vs. 2 h after blast TBI

The third comparison, between samples at 24 h and 2 h after blast injury, showed that 39 genes are differentially expressed: increased expression of 20 genes and decreased expression of 19 genes in injured animals. The most noticeable alteration was in immune related genes, which showed differential expression of 10 genes: 4 genes (3 complement-related genes and 1 IgG-related gene) were upregulated and 6 genes (IL-1β, IL-1α, and chemokine motifs) were downregulated at 24 h compared to 2 h post injury. Also, increases in genes for various secreted extracellular proteins occurred at 24 h compared to 2 h after blast injury, including proteins involved in iron trafficking (Lcn2), endocrine (Trh), and function as protease inhibitors (A2m, Spin2c, Serping1). Several membrane associated genes were also upregulated at 24 h vs 2 h, including those involved in receptor function (Bzrp), membrane adhesion (Cd44), and cell-cell interaction (Emp3).

Multiplex assessment of cytokines, chemokines, and growth factors

At 2 h after injury, three cytokines and one chemokine exhibited significant increases (Figure 3A, B). Levels of IL-1α increased by ~3-fold vs sham (1.3±0.4 pg/mg protein vs. 3.5±0.6 pg/mg protein; $p<0.05$). Levels of IL-6 also increased ~3-fold vs sham (5.5±0.6 pg/mg protein vs. 13.4±2.0 pg/mg protein; $p< 0.05$). Levels of IL-12p70 increased ~2-fold vs sham (8.3±1.9 pg/mg protein vs. 16.9±2.2 pg/mg protein; $p< 0.05$). The chemokine MIP-1α showed the greatest increase with undetectable levels in shams and 5.12±1.54 pg/mg protein in injured cortex ($p < 0.05$). One additional cytokine, chemokine, and growth factor, IL-10 ($p = 0.078$), GRO/KC ($p = 0.072$), and VEGF ($p = 0.055$) showed at least 2-fold greater levels after blast-injury vs sham, but, these did not reach statistical significance.

At 24 h after blast injury, all cytokine levels (IL-1α, IL-6, and IL-12p70) returned to values that were not different from sham (Figure 3C, D). However, the chemokine MIP-1α continued to demonstrate a significant increase vs respective sham (Figure 3C).

Markers of oxidative stress and damage

Blast TBI produced significant decrease (~30% reduction vs sham control) in reduced glutathione in the hippocampus ipsilateral to the blast exposure at 2 h and 24 h after the insult ($p < 0.05$, Figure 4A). In addition, low molecular weight thiols were significantly reduced (~15-20%) vs sham control at both 2 and 24 h after blast injury ($p < 0.05$, Figure 4B). Protein thiols were significantly reduced vs. sham at 24 h after injury (Figure 4C), although there was also a trend toward reduction at 2 h ($p = 0.052$, Figure 4C). Ascorbate levels in hippocampus ipsilateral to blast exposure were not significantly decreased vs. respective sham, although a trend toward reduction (~30%) was again seen at 2 h ($p = 0.08$, Figure 4D). Screening for formation of 4-hydroxynoneanl adducts as evidence of lipid peroxidation on western blot revealed that they were present at 24 h but not 2 h after blast exposure (Figure 4E).

ATP, purine metabolites and adenosine

As shown in Figure 5A-G, no statistically significant changes in brain levels of ATP, ADP, 5'-AMP, 2'-AMP, 3',5'-cAMP, adenosine or inosine were observed. Neither 2',3'-cAMP nor 3'-AMP were detected. When the control, 2-h injury; 24-h injury; and lethal exposures (rats that died from acute hypoxemia from impact apnea) were regressed, adenosine levels in brain tissue were not associated with 5'-AMP but were highly correlated with 2'-AMP, Figures 5 H, I, respectively) suggesting that adenosine after blast TBI is derived from 2'-AMP.

Discussion

Despite a blast exposure with body shielding and fixation of the head to minimize any acceleration, and using an injury level that mimicked the human condition reported in uncomplicated blast exposure – i.e., producing neurological damage largely restricted axonal injury in the deep white matter,[1,26,27] we noted robust biochemical and molecular alterations of TBI-related secondary injury pathways in hippocampus and cortex in both hemispheres. We have also examined brain sections from our prior report[11] in this model for Tau staining after injury using AT8 and a pan-tau immunostaining and did not identify this protein up to two weeks post-blast, indicating that this insult is below the threshold required for acute Tau deposition (Data not shown). Our findings, thus, support the hypothesis that mild to moderate uncomplicated blast exposure limited to brain can induce a robust biochemical and molecular features of the secondary injury response in rat brain.

Gene Array

Changes in gene array reflected tissue alterations in the hippocampus ipsilateral to the exposure. We reported in this model that neuronal death in CA1was rare but there were consistent alterations of dendrites assessed by cupric silver staining in multiple hippocampal subfields.[11] These changes were similar both ipsi- and contralateral to blast exposure and were greatest between 24 h and 72 h.

The most obvious changes in the gene array at 2 h were increases in 7 ribosomal proteins (Rps10, Rpl29, Rpl35, Rpl41, Rps14, Rpl32, Rps26). Similar increases were noted at 4 h after controlled cortical impact (CCI),[28] a much more highly characterized rat model of TBI than blast exposure. Since ribosomal proteins regulate transcription and translation, the early increase may support acute upregulation of various proteins after injury.

We also noted that three genes involved in mitochondrial respiration and electron transport (cytochrome oxidase 7b [COX7b], Ndufa11, Uqcrh) were upregulated. COX7b is a component of COX that may have a role in assembly of the protein while Ndufa 11 is liked to mitochondrial complex I.[29] Sajja et al[30] reported decreases in succinate, and other metabolites consistent with mitochondrial stress in hippocampus of rats exposed to blast (shock tube, ~17 PSI). Hemoglobin alpha and beta chain (Hbb, Hba-a1) were also upregulated at 4 h. This mirrors the work of Natale et al[31] in fluid percussion injury (FPI) and may reflect local tissue hypoxia, since apnea accounted for 25-27 % acute mortality in our model[11] and is seen after FPI. However, downregulation of mitochondrial genes has been reported by others at 3-4 h after CCI,[32,33] contrasting our findings. Thus, unlike the prior reports of downregulation of mitochondrial genes in CCI, we noted general upregulation of mitochondrial metabolic genes at 2h. This could reflect our sampling time, differences in injury level, or a unique profile for blast.

At 24 h after blast injury, the greatest increases in gene expression were seen in two astrocyte proteins, GFAP and vimentin, and the inflammatory protein complement component 1. Increase in gene expression of astrocyte markers at 24 h mirrors other reports using proteomics or imunohistochemistry.[30,34,35] In the CCI model in rats, GFAP and vimentin, assessed by 2-D gel, also showed large increases in hippocampus.[36] Astrocytes play a neuroprotectant after CCI,[37] however, their role in blast TBI is undefined. Gao et al[38] reported increases in complement component 1 after TBI in human cerebrospinal fluid (CSF) via 2D gel, suggesting that it is highly expressed after injury. It signals leukocyte recruitment.

At 24 h, genes involved in differentiation, neurogenesis, growth (Gap43, Prss11), apoptosis and the stress response (Hspb1, Mt1a, Anxa3) were upregulated vs. sham. Natale et al[31] reported similar increases in metallothionine and another member of the heat shock protein family Hsp70 at 4-24 h after FPI in rats. Increases in Mt and Hsp gene expression could also reflect a response to acute blood-brain barrier (BBB) injury and a stress response, respectively.

Upregulation of Gap43 and Prss 11 could reflect increased extracellular signaling in hippocampus, possibly due to neurite outgrowth. We previously reported cortical BBB injury in our model at 24 h; however, BBB alterations in the hippocampus were not seen.[11]

There was increased expression of genes involved in transport function (solute carrier family 3 and 25, mitochondrial membrane ATP synthase, Dncic1, Nsf) at 24 h. Increased function of genes such as Dncic1 would support dynein associated organelle transport, and solute carrier family 25 and 3 would support transport of ATP and amino acids. These transport functions may serve processes such as cellular signaling and remodeling after injury. However, other transport function associated genes (Atp6v0c, Sv2b, Laptm4a, Atp2a2) were downregulated at 24 h, suggesting a differential modulation of various transport functions.

There was also increased expression of genes involved in glycolysis and oxidative phorphorylation (Uqcrc2, Mdh1, Gpi, Aldoa) at 24 h.

Calcium signaling-associated genes were downregulated at 24 h (Camk2n1, Camk2b, calreticulin). Downregulation of CaMKII has been reported after CCI.[32] Calcium dependent signaling may be beneficial or detrimental after injury.[39,40]

The most obvious change in gene expression at 24 h vs.2 h was differential expression of 10 immune response related genes: 4 genes (3 complement related genes and 1 IgG related gene) were upregulated and 6 genes (IL-1β, IL-1α, chemokine motifs) were downregulated. Complement and IgG upregulation are integral to the acute phase response. However, downregulation of IL-1β, IL-1α, and chemokines at 24 h vs. 2 h suggests recovery after an early inflammation. An early increase in IL-1 α with recovery by 24 h corroborates our protein data (see below). However, the delayed downregulation in chemokine gene expression contrasts our protein data which showed sustained increases in cortex. The delayed decrease in chemokine gene expression may thus represent feedback inhibition.

Increases in genes for various secreted extracellular proteins were seen at 24 h vs 2 h. These proteins regulate iron trafficking (Lcn2), endocrine effects (Trh), and function as protease inhibitors (A2m, Spin2c, Serping1). Thus there is an increase in expression of genes for extracellularly secreted proteins at 24 h vs. 2 h. Several membrane associated genes were also upregulated including those involved in receptor function (Bzrp), membrane adhesion (Cd44), and cell-cell interaction (Emp3). Finally, downregulation of several differentiation and growth related genes (Ndrg2, Rtn4, Cspg5) was seen at 24 h vs. 2 h.

Multiplex analysis of cytokines, chemokines and growth factors

Multiplex cytokine analysis has been applied to rat brain tissue in non-blast models with excellent correlation to gold standard ELISA.[40] Prior work in CNS injury has shown varied cytokine patterns depending on the injury mechanism. Takamiya et al[42] applied a 27-plex over 240 h after stab wound and noted elevations of pro-inflammatory cytokines (IL-1α, IL-1β, IL-6, IL-12p40, IL-12p70, IL-18, TNF-α), anti-inflammatory cytokines (IL-5, IL-10), and chemokines (G-CSF, GRO/KC, MIP-2) at various time points. Buttram et al[43] applied multiplex to CSF of TBI patients and noted increases of pro-inflammatory cytokines (IL-1β, IL-6, and IL-12p70), an anti-inflammatory cytokine (IL-10), and chemokines (IL-8, MIP-1α). In adult human brain tissue from patients who died from TBI, Frugier et al[44] noted a rapid increase in IL-1β, IL-6, IL-8 and TNF-α. We found a somewhat unique brain tissue cytokine pattern after blast-TBI, with rapid increases of the chemokine MIP-1α, and pro-inflammatory cytokines IL-1α, IL-6, and IL-12p70 at 2 h, and a sustained elevation of MIP-1α at 24 h. Unlike other forms of TBI, anti-inflammatory cytokines were not increased. Our data mirror those of Kwon et al[34] who reported increases in IL-6 in pre-frontal cortex and hippocampus of rats exposed to blast TBI (shock tube) with concurrent predator stress to mimic battlefield conditions.

MIP-1α is a β- (or CC) chemokine[45] stimulating macrophage infiltration at injury sites. It is produced in white matter lesions in multiple sclerosis and associated with microglial

activation.[46] MIP-1α is elevated in CSF at 24 h after clinical TBI.[43] After olfactory bulb axotomy in mice, MIP-1α was markedly increased at 3 d and regulated dendritic cell migration.[47] Fe2+-mediated free radical production and free ATP via purinergic $P2X_7$ receptors initiate MIP-1α expression[48]–which could thus be relevant to blast TBI. No increase in MIP-1α was seen after a mouse stab-wound suggesting differences between blast and penetrating TBI.[42]

Surprisingly, we noted an increase of IL-1α at 2 h, but not IL-1β. This corroborates our gene array data. IL-1α and IL-1β are agonists for type 1 and type 2 IL-1 receptors. In glia, IL-1-receptor activation by either agonist triggers activation of mitogen activated protein kinases and nuclear factor kappa B.[49] Lemke et al[50] showed that after LPS/IFNγ injection, IL-1α and IL-1β are induced in peri-lesional microglia. IL-1β, but not IL-1α, also induces nerve growth factor,[51] which can be neuroprotective. While both cytokines can induce chemokines, only IL-1β induces IL-6 expression.[52] IL-1α associates with nuclear chromatin and is released after necrotic cell death and incites inflammation.[53] IL-1α but not IL-1 ILβ is released by platelets after vascular injury and initiates chemokine release by endothelium.[54] Given, the role of vascular injury in blast TBI, this theoretical mechanism bears further study and might contribute to vascular dysfunction after blast TBI. Despite the lack of an IL-1β elevation, we noted an increase of IL-6 after blast-TBI. IL-6 is elevated in CSF after clinical TBI.[55,56] It can act as a neuronal survival factor[55] and/or as a chemokine.[57] Further study is needed to determine if IL-6 is neuroprotective in blast-TBI, or inciting further inflammation.

IL-12 stimulates CD4+ T-cells to acquire a pro-inflammatory Th1 phenotype[58] and is elevated in CSF after TBI in humans.[43] However, injection of IL-12 into lesioned spinal cord causes neurogenesis and remeylination in mice.[59] Given the degree of axonal injury in blast TBI, further study is needed to determine if IL-12p70 facilitates myelin repair after axonal injury.

In light of the link between neuroinflammation and CTE,[25] our gene array and Multiplex data suggest that blast TBI, even at an injury level below that needed to yield appreciable cell

death, APP accumulation, or acute Tau accumulation, initiates a neuro-inflammatory response that includes acute cytokine and more prolonged chemokine elevation. The long-term consequences of blast TBI at this injury level could be important with regard to neuroinflammation and CTE. It is certainly unclear if one would anticipate immediate or more delayed Tau deposition after blast TBI. Further study is needed in this regard.

Markers of oxidative stress

Blast TBI produced a significant decrease in both reduced GSH and LMWT in the hippocampus ipsilateral to exposure to a degree similar to that seen in the CCI model of TBI in rats at a moderate injury level. A 31% reduction in GSH was seen at 24 h in CCI.[60] This is surprising given that neuronal death was rare in hippocampus in this model.[11] However, a consistent pattern of synapse or terminal degeneration was seen in hippocampus in that report assessed by silver staining. Cernak et al[10] reported cytoplasmic vacuoles and expanded perineural spaces on electron microscopic assessment in the hippocampus of rats exposed 24 h earlier to whole body or local chest blast TBI (shock tube; ~49 PSI) and an ~50% increase in the lipid peroxidation marker malondialdehyde was also seen. Cernak et al[10] also noted an ~30-40% reduction of GSH that recovered by 5 d. Our results build upon that work by showing that head only blast exposure produces a similar level of oxidative stress in hippocampus as either the whole body or body-only exposure. It is remarkable that these three divergent approaches each produced subtle hippocampal neuropathology and substantive evidence of oxidative stress.

Ascorbate levels in hippocampus ipsilateral to blast exposure were not significantly decreased vs. sham, and although a trend toward reduction (~30%) was seen, it suggests that the oxidative stress in our blast-TBI model is somewhat less in magnitude than that seen in CCI, where significant reductions in ascorbate were seen.[60] Studies of CSF ascorbate levels in humans with severe TBI show marked and sustained depletion.[61] However, the effect of mild

TBI on ascorbate in human TBI remains undefined. Nevertheless, our data suggest that oxidative stress is an important therapeutic target even in mild blast TBI. Our data also suggest that caution is in order with regard to the use of hyperbaric oxygen in blast TBI, particularly early after exposure. They also suggest the need to study therapies targeting oxidative stress.

ATP, Purines, and Adenosine

Blast injury did not alter brain tissue levels of ATP, ADP or 5'-AMP, suggesting that our mild insult did not induce energy failure. This is consistent with the fact that we previously reported axonal injury rather than neuronal death, and argues against a major role for ischemia in the initial 24 h. Although 5'-AMP (produced from ATP/ADP metabolism) is considered the major precursor for adenosine, recent studies suggest that adenosine may also derive from the metabolism of 2',3'-cAMP to 3'-AMP or 2-AMP with subsequent metabolism to adenosine.[24] Our current study reveals that brain tissue levels of adenosine are strongly associated with 2'-AMP but not 5'-AMP, consistent with 2'-AMP as a source of adenosine in the injured brain. It has been shown that 2, 3 cAMP is produced from the poly-A tails in the breakdown cellular mRNA.[24] Thus, adenosine levels after even relatively mild blast TBI are correlated with brain tissue levels of 2'-AMP, suggesting that mRNA breakdown occurs and may drive the production of the neuroprotectant adenosine. Additional studies are warranted to address this hypothesis.

Limitations

Our sample size was limited; however, this study was designed as a screening study to direct future definitive mechanistic investigation. Thus, we believe it is valuable, particularly given the expertise in blast physics and modeling that guided the work, and the comprehensive neuropathological evaluation we previously reported.[11] Given the different methodological requirements for the many assays used in this study, and limitations of tissue sample volume, it could have compromised the assays to try to carry out all of them in each brain region. Also, in

that these studies were carried out before the neuropathology had been defined—it was unclear where the most damage would be seen. Since our model results in global injury, our findings can direct future work. However, since axonal injury was greatest in cerebellum and brainstem, these regions should be evaluated in the future. It will also be important to extend these studies to >24 h after injury. Our model is associated with ~25% mortality from impact apnea, providing some insight into severity. However, characterization of behavioral deficits is needed to make appropriate correlations. We did not video record head movement. The head was the only part of the rat that was exposed and it was constrained to prevent acceleration. However, given recent findings,[2] the role of head acceleration should be explored. We included anesthesia controls; additional controls such as rats exposed to blast noise could also be informative.[62] We purposefully sought to eliminate extracerebral blast exposure using body protection, but this does not preclude effects of extracerebral blast on CNS-injury. Finally, study of repeated blast TBI deserves attention in light of its importance.

Conclusions

Our mechanistic screening study strongly suggests a marked astrocytic response, neuro-inflammation including both cytokines and chemokines, and oxidative stress after blast-induced TBI in rats produced by a shock tube exposure of ~35 PSI. In recent studies of a large animal model as a part of PREVENT a significant increase in GFAP positive astrocyte expression has also been reported.[6] These findings were seen in the setting of blast exposure 1) limited to the head, 2) with head constraint to limit acceleration, and 3) a relatively mild injury that is associated primarily with axonal and fiber tract injury seen only with cupric silver staining. Our data argue against a role for energy failure early after injury and suggest that the 2, 3 cAMP pathway may be involved. Finally, pattern analysis on gene array suggests similarities in the response to those seen in both Alzheimer disease and long-term potentiation, conditions intimately linked to memory processing and/or disturbances in memory function. Our studies provide clues for further exploration of mechanistic alterations and therapeutic testing in experimental blast TBI.

Acknowledgement

Supported by DARPA PREVENT (N660001-10-C2124). We thank Keri Janesko-Feldman and Jeremy Henchir for technical support. We thank Marci Provins and Fran Mistrick for manuscript preparation. Microarray data were generated by the Genomics Core Laboratory, University of Pittsburgh, and statistical analyses were performed by the GPCL-Bioinformatics Analysis Core (GPCL-BAC), University of Pittsburgh. We thank Dr. James Lyons-Weiler for his valuable assistance. “The views, opinions, and/or findings contained in this article are those of the author and should not be interpreted as representing the official views or policies either expressed or implied of the Defense Advanced Research Projects Agency or the Department of Defense. Approved for public release, distribution unlimited.”

References

1. MacDonald, C.L., Johnson, A.M., Cooper, D., Nelson, E.C., Werner, N.J., Shimony, J.S., Snyder, A.Z., Raichle, M.E., Witherow, J.R., Fang, R., Flaherty, S.F., and Brody, D.L. (2011). Detection of blast-related traumatic brain injury in U.S. military personnel. N. Engl. J. Med. 364, 2091-2100.

2. Goldstein, L.E., Fisher, A.M., Tagge, C.A., Zhang, X.L., Velisek, L., Sullivan, J.A., Upreti, C., Kracht, J.M., Ericsson, M., Wojnarowicz, M.W., Goletiani, C.J., Maglakelidze, G.M., Casey, N., Moncaster, J.A., Minaeva, O., Moir, R.D., Nowinski, C.J., Stern, R.A., Cantu, R.C., Geiling, J., Blusztajn, J.K., Wolozin, B.L., Ikezu, T., Stein, T.D., Budson, A.E., Kowall, N.W., Chargin,D., Sharon, A., Saman, S., Hall, G.F., Moss, W.C., Cleveland, R.O., Tanzi, R.E., Stanton, P.K., and McKee, A.C. (2012). Chronic traumatic encephalopathy in blast-exposed military veterans and a blast neurotrauma mouse model. Sci. Transl. Med. 4, 134ra60; DOI: 10.1126/scitranslmed.3003716.

3. Koliatsos, V.E., Cernak, I., Xu, L., Song, Y., Savonenko, Al, Crain, B.J., Eberhart, C.G., Frangakis, C.E., Melnikova, T., Kim, H, and Lee, D. (2011). A mouse model of blast injury to brain: Initial pathological, neuropathological, and behavioral characterization. J. Neuropathol. Exp. Neurol. 70, 399-416.

4. Long, J.B., Bentley, T.L., Wessner, K.A., Cerone, C., Sweeney, S., and Bauman, R.A. (2009). Blast overpressure in rats: Recreating a battlefield injury in the laboratory. J. Neurotrauma 26, 827-840.

5. Bauman, R.A., Ling, G., Tong, L., Januszkiewicz, A., Agoston, d., Delanerolle, N., Kim, Y., Ritzel, D., Bell, R., Ecklund, J., Armonda, R., Bandak, F., and Parks, S. (2009). An introductory characterization of a combat-casualty-care relevant swine model of

closed head injury resulting from exposure to explosive blast. J. Neurotrauma 26, 841-860.

6. de Lanerolle, N.C., Bandak, F.A., Kang, D., Li, A.Y., Du, F., Swauger, P., Parks, S. Ling, G., and Kim, J.H. (2011). Characteristics of an Explosive Blast-Induced Brain Injury in an Experimental Model. J Neuropathol Exp Neurol Vol. 70, No. 11, 1046-1057.

7. Readnower, R.D., Chavko, M., Adeeb, S., Conroy, M.D., Pauly, J.R., McCarron, R.M., and Sullivan, P.G. (2010). Increase in blood brain barrier permeability, oxidative stress, and activated microglia in a rat model of blast induced traumatic brain injury. J. Neurosci. Res. 88, 3530-3539.

8. Svetlov, S.I., Prima, V., Kirk, D.R., Gutierrez, H., Curley, K.C., Hayes, R.L., and Wang, K.K.W. (2010). Morphologic and biochemical characterization of brain injury in a model of controlled blast overpressure. J. Trauma 69, 795-804.

9. Lu, J., Ng, K.C., Ling, G., Wu, J., Poon, D.J.F., Kan, E.M., Tan, M.H., Wu, Y.J., Li, P., Moochhala, S., Yap, E., Lee, L.K.H., Teo, M., Yeh, I.B., Sergio, D.M.B., Chua, F., Kumar, S.D., and Ling, E.A. (2012). Effect of exposure on the brain structure and cognition in Macaca fascicularis. J. Neurotrauma 29, 1434-1454.

10. Cernak, I., Wang, Z., Jiang, J., Bian, X., and Savic, J. (2001). Ultrastructural and functional characteristics of blast injury-induced neurotrauma. J. Trauma 50, 695-706.

11. Garman, R.H., Jenkins, L.W., Switzer, R.C., Bauman, R.A., Tong, L.C., Swauger, P.V., Parks, S.A., Dixon, C.E., Clark, R.S.B., Bayır, H., Kagan, V., Jackson, E.K., and Kochanek, P.M. (2011). Blast exposure injury in rats with body protection is characterized primarily by diffuse axonal injury. J. Neurotrauma 28, 947-959.

12. Levin, H.S., Wilde, E., Troyanskaya, M., Peterson, N.J., Scheibel, R., Newsome, M., Radaideh, M., Wu, T., Yallampalli, R., Chu, Z., and Li, X. (2010). Diffusion tensor imaging of mild to moderate blast-related traumatic brain injury and its sequelae. J. Neurotrauma 27, 683-694.

13. Scheibel, R.S., Newsome, M.R., Troyanskaya, M., Lin, X., Steinberg, J.L., Radaideh, M., and Levin, H.S. (2012). Altered brain activation in military personnel with one or more traumatic brain injuries following blast. J. Int. Neuropsychol. Soc. 18, 89-100.

14. Risling, M., Plantman, S., Angeria, M., Rostami, E., Bellander, B.-M., Kirkegaard, M., Arborelius, U., and Davidsson, J. (2011). Mechanisms of blast induced brain injuries, experimental studies in rats. Neuroimage 54, S89-S97.

15. Elder, G.A., Dorr, N.P., De Gasperi, R., Sosa, M.A.G., Shaughness, M.C., Maudlin-Jeronimo, E., Hall, A.A., McCarron, R.M., and Ahlers, S.T. (2012). Blast exposure induces post traumatic stress disorder-related traits in a rat model of mild traumatic brain injury. J. Neurotrauma [Epub ahead of print].

16. Cernak, I. (2010). The importance of systemic response in the pathobiology of blast-induced neurotrauma. Front. Neurol. 1, 151.

17. Ling, G., Bandak, F., Armonda, R., Grant, G., and Ecklund, J. (2009). Explosive blast neurotrauma. J. Neurotrauma 26, 815-825.

18. Armonda, R.A., Bell, R.S., Vo, A.H., Ling, G., DeGraba, T.J., Crandall, B., Ecklund, J., and Campbell, W.W. (2006). Wartime traumatic cerebral vasospasm: Recent review of combat casualties. Neurosurgery 59, 1215-1225.

19. Jordan, B.R. (2004). How consistent are expression chip platforms? Bioessays 26, 1236-1242.

20. Patel, S., and Lyons-Weiler, J. (2004). caGEDA: A web application for the integrated analysis of global gene expression patterns in cancer. Appl. Bioinformatics 3, 49-62.

21. Draghici, S., Khatri, P., Tarca, A.L., Amin, K., Done, A., Voichita, C., Georgescu, C., and Romero, R. (2007). A systems biology approach for pathway level analysis. Genome Res. 17, 1537-1545.

22. Bayır, H., Tyurin, V.A., Tyurina, Y.Y., Viner, R., Ritov, V., Amoscato, A.A., Zhao, Q., Zhang, X.J., Janesko-Feldman, K.L., Alexander, H., Basova, L.V., Clark, R.S., Kochanek, P.M., and Kagan, V.E. (2007). Selective early cardiolipin peroxidation after traumatic brain injury: An oxidative lipidomics analysis. Ann. Neurol. 62, 154-169.

23. Belikova, N.A., Glumac, A.L., Kapralova, V., Tyurina, Y.Y., Kochanek, P.M., Kagan, V.E., and Bayır, H. (2011). A high-throughput screening assay of ascorbate in brain samples. J. Neurosci. Methods 201, 185-190.

24. Jackson, E.K., Ren, J., and Mi, Z. (2009). Extracellular 2',3'-cAMP is a source of adenosine. J. Biol. Chem. 284, 33097-33106.

25. DeKosky, S.T., Ikonomovic, M.D., and Gandy, S. (2010). Traumatic brain injury—football, warfare, and long-term effects. N. Engl. J. Med. 363, 1293-1296.

26. Morey, R.A., Haswell, C.C., Selgrade, E.S., Massoglia, D., Liu, C., Weiner, J., Marx, C.E., Cernak, I., and McCarthy, G.; MIRECC Work Group. (2012). Effects of chronic mild traumatic brain injury on white matter integrity in Iraq and Afghanistan war veterans. Hum. Brain Mapp. 2012 Jun 15 [Epub ahead of print].

27. Bazarian, J.J., Donnelly, K., Petersen, D.R., Warner, G.C., Zhu, T., and Zhong, J. (2012). The relation between posttraumatic stress disorder and mild traumatic brain injury acquired during operations Enduring Freedom and Iraqi Freedom: A diffusion tensor imaging study. J. Head Trauma Rehabil. 2012 May 28. [Epub ahead of print].

28. Yoshiya, K., Tanaka, H., Kasai, K., Irisawa, T.,Shiozaki, T., and Sugimoto, H. (2003). Profile of gene expression in the subventricular zone after traumatic brain injury. J. Neurotrauma 20, 1147-1162.

29. Berger, I., Hershovitz, E., Shaag, A., Edvardson, S. Saada, A., and Elpeleg, O. (2008). Mitochondrial complex I deficiency caused by a deleterious NDUFA11 mutation. Ann. Neurol. 63, 405-408.

30. Sajja, V.S.S.S., Galloway, M.P., Ghoddoussi, F., Thiruthalinathan, D., Kepsel, A., Hay, K., Bir, C.A., and VandeVord, P.J. (2012). Blast-induced neurotrauma leads to neurochemical changes and neuronal degeneration in the rat hippocampus. NMR Biomed. DOI: 10.1002/nbm.2805.

31. Natale, J.E., Ahmed, F., Cernak, I., Stoica, B., and Faden, A.I. (2003). Gene expression profile changes are commonly modulated across models and species after traumatic brain injury. J. Neurotrauma 20, 907-927.

32. Matzilevich, D.A., Rall, J.M., Moore, A.N., Grill, R.J., and Dash, P.K. (2002). High-density microarray analysis of hippocampal gene expression following experimental brain injury. J. Neurosci. Res. 67, 646-663.

33. Long, Y., Zou, L., Liu, H., Lu, H.,Yuan, X., Robertson, C.S., and Yang, K. (2003). Altered expression of randomly selected genes in mouse hippocampus after traumatic brain injury. J. Neurosci. Res. 71, 710-720.

34. Kwon, S.-K.C, Koveski, E., Gyorgy, A.B., Wing, D., Kamnaksh, A., Walker, J., Long, J.B., and Agoston, D.V. (2011). Stress and traumatic brain injury: A behavioral, proteomics, and histological study. Frontiers in Neurology 2, Article 12.

35. Svetlov, S.I., Prima, V., Glushakova, O., Svetlov, A, Kirk, D.R., Gutierrez, H., Serebruany, V.L., Curley, K.C., Wang, K.K.W., and Hayes, R.L. (2012). Neuro-glial and systemic mechanisms of pathological responses in rat models of primary blast overpressure compared to “composite” blast. Fronts in Neurology 3, Article 15.

36. Kochanek, A.R., Kline, A.E., Gao, W.M., Chadha, M., Lai, Y., Clark, R.S., Dixon, C.E., and Jenkins, L.W. (2006). Gel-based hippocampal proteomic analysis 2 weeks following traumatic brain injury to immature rats using controlled cortical impact. Dev. Neurosci. 28, 410-419.

37. Myer, D.J., Gurkoff, G.G., Lee, S.M., Hovda, D.A., and Sofroniew, M.V. (2006). Essential protective roles of reactive astrocytes in traumatic brain injury. Brain 129, 2761-2772.

38. Gao, W., Chadha, M.S., Berger, R.P., Omenn, G., Allen, D., Pisano, M., Adelson, P.D., Clark, R.S.B., Jenkins, L.W., and Kochanek, P.M. (2007). Biomarkers and diagnosis: A gel-based proteomic comparison of human cerebrospinal fluid between inflicted and non-inflicted pediatric traumatic brain injury. J. Neurotrauma 24, 43-53.

39. Zalewska, T., Zablocka, B., and Domanska-Janik, K. (1996). Changes of Ca2+/calmodulin-dependent protein kinase-II after transient ischemia in gerbil hippocampus. Acta Neurobiol. Exp. (Wars). 56, 41-48.

40. Waxham, M.N., Grotta, J.C., Silva, A.J., Strong, R., and Aronowski, J. (1996). Ischemia-induced neuronal damage: A role for calcium/calmodulin-dependent protein kinase II. J. Cereb. Blood Flow Metab. 16, 1-6.

41. Hulse, R.E., Kunkler, P.E., Fedynyshyn, J.P., and Kraig, R.P. (2004). Optimization of multiplexed bead-based cytokine immunoassays for rat serum and brain tissue. J. Neurosci. Methods 136, 87-98.

42. Takamiya, M., Fujita, S., Saigusa, K., and Aoki, Y. (2007). Simultaneous detections of 27 cytokines during cerebral wound healing by multiplexed bead-based immunoassay for wound age estimation. J. Neurotrauma 24, 1833-1844.

43. Buttram, S.D., Wisniewski, S.R., Jackson, E.K., Adelson, P.D., Janesko-Feldman, K., Bayır, H., Berger, R.P., Clark, R.S.B., and Kochanek, P.M. (2007). Multiplex assessment of cytokine and chemokine levels in cerebrospinal fluid following severe pediatric traumatic brain injury: Effects of moderate hypothermia. J. Neurotrauma 24, 1707-1718.

44. Frugier, T., Morganti-Kossmann, M.C., O'Reilly, D., and McLean, C.A. (2010). In situ detection of inflammatory mediators in post mortem human brain tissue after traumatic brain injury. J. Neurotrauma 27, 497-507.

45. DiPietro, L.A., Burdick, M., Low, Q.E., Kunkel, S.L., and Strieter, R.M. (1998). MIP-1alpha as a critical macrophage chemoattractant in murine wound repair. J. Clin. Invest. 101, 1693-1698.

46. Balashov, K.E., Rottman, J.B., Weiner, H.L., and Hancock, W.W. (1999). CCR5(+) and CXCR3(+) T cells are increased in multiple sclerosis and their ligands MIP-1alpha and IP-10 are expressed in demyelinating brain lesions. Proc. Natl. Acad. Sci. U.S.A. 96, 6873-6878.

47. Zozulya, A.L., Reinke, E., Baiu, D.C., Karman, J., Sandor, M., and Fabry, Z. (2007). Dendritic cell transmigration through brain microvessel endothelium is regulated by MIP-1alpha chemokine and matrix metalloproteinases. J. Immunol. 178, 520-529.

48. Kataoka, A., Tozaki-Saitoh, H., Koga, Y., Tsuda, M., and Inoue, K. (2009). Activiation of P2X7 reeptors induces CCL3 production in microglial cells through transcription factor NFAT. J. Neurochem. 108, 115-125.

49. Andre, R., Pinteaux, E., Kimber, I., and Rothwell, N.J. (2005). Differential actions of IL-1 alpha and IL-1 beta in glial cells share common Il-1 signalling pathways. Neuroreport 16, 153-157.

50. Lemke, R., Hartlage-Rübsamen, M., and Schliebs, R. (1999). Differential injury-dependent glial expression of interleukins-1 alpha, beta, and interleukin-6 in rat brain. Glia 27, 75-87.

51. DeKosky, S.T., Styren, S.D., O'Malley, M.E., Goss, J.R., Kochanek, P.M., Marion, D., Evans, C.H., and Robbins, P.D. (1996). Interleukin-1 receptor antagonist suppresses neurotrophin response in injured rat brain. Ann. Neurol. 39, 123-127.

52. Tsaikir, N., Kimber, I., Rothwell, N.J., and Pinteaux, E. (2008). Differential effects of interleukin-1 alpha and beta on interleukin-6 and chemokine synthesis in neurons. Mol. Cell. Neurosci. 38, 259-265.

53. Cohen, I., Rider, P., Carmi, Y., Braiman, A., Dotan, S., White, M.R., Voronov, E., Martin, M.U., Dinarello, C.A., and Apte, R.N. (2010). Differential release of chromatin-bound IL-1alpha discriminates between necrotic and apoptotic cell death by the ability to induce sterile inflammation. Proc. Natl. Acad. Sci. U.S.A. 107, 2574-2579.

54. Thornton, P., McColl, B.W., Greenhalgh, A., Denes, A., Allan, S.M., and Rothwell, N.J. (2010). Platelet interleukin-1alpha drives cerebrovascular inflammation. Blood 115, 3632-3639.

55. Kossmann, T., Hans, V., Imhof, H.G., Trentz, O., and Morganti-Kossmann, M.C. (1996). Interleukin-6 released in human cerebrospinal fluid following traumatic brain injury may trigger nerve growth factor production in astrocytes. Brain Res. 713, 143-152.

56. Bell, M., Kochanek, P.M., Doughty, L.A., Carcillo, J.A., Adelson, P.D., Clark, R.S.B., Wisniewski, S.R., Whalen, M.J., and DeKosky, S.T. (1997). Interleukin-6 and Interleukin-10 in cerebrospinal fluid after traumatic brain injury in children. J. Neurotrauma 14, 451-457.

57. Clahsen, T., and Schaper, F. (2008). Interleukin-6 acts in the fashion of a classical chemokine on monocytic cells by inducing integrin activation, cell adhesion, actin polymerization, chemotaxis, and transmigration. J. Leukoc. Biol. 84, 1521-1529.

58. Trinchieri, G. (1995). Interleukin-12: A pro-inflammatory cytokine with immunoregulatory functions that bridge innate resistance and antigen-specific adaptive immunity. Annu. Rev. Immunol. 13, 251-276.

59. Yaguchi, M., Ohta, S., Toyama, Y., Kawakami, Y., and Toda, M. (2008). Functional recovery after spinal cord injury in mice through activation of microglia and dendritic cells after IL-12 administration. J. Neurosci. Res. 86, 1972-1980.

60. Tyurin, V.A., Tyurina, Y.Y., Borisenko, G.G., Sokolova, T.V., Ritov, V.B., Quinn, P.J., Rose, M., Kochanek, P., Graham, S.H., and Kagan, V.E. (2000). Oxidative stress following traumatic brain injury in rats: Quantitation of biomarkers and detection of free radical intermediates. J Neurochem 75, 2178-2189.

61. Bayır, H., Kagan, V.E., Tyurina, Y.Y., Tyurin, V.A., Ruppel, R.A., Adelson, P.D., Graham, S.H., Janesko, K., Clark, R.S.B., and Kochanek, P.M. (2002). Assessment of antioxidant reserve and oxidative stress in cerebrospinal fluid after severe traumatic brain injury in infants and children. Pediatr. Res. 51, 571-578.

62. Kamnaksh, A., Kovesdi, E., Kwon, S.K., Wingo, d., Ahmed, F., Grunberg, N.E., Long, J., and Agoston, D.V. (2011). Factors affecting blast traumatic brain injury. J. Neurotrauma 28, 2145-2153.

Figure Legends

Figure 1

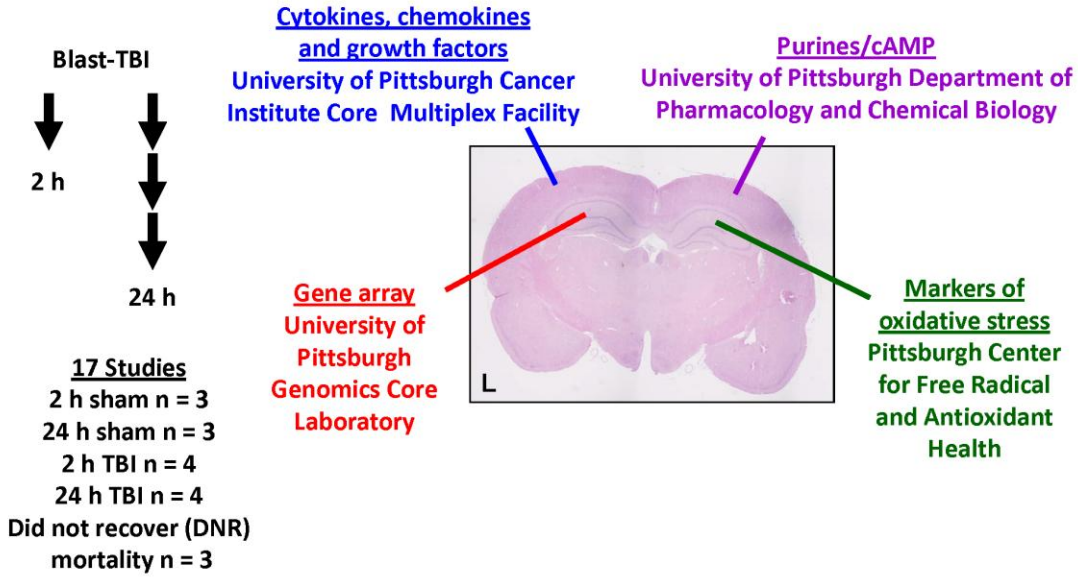

Figure 1. Overall study design for screening biochemical and molecular mechanisms of secondary injury and repair after experimental blast induced TBI (helium-driven shock tube) in rats using a model previously characterized for neuropathology.[11] Studies were carried out in rats exposed to blast TBI (35 PSI, with body protection, and head restraint) with the left side of the head facing the shock-wave exposure. At 2 h or 24 h after either blast or sham anesthesia exposure, rats were sacrificed and brain tissue samples were rapidly harvested and snap frozen. Samples were obtained from left (L) and right hippocampus and pre-frontal cortex. Each brain region was used for a separate molecular or biochemical assay as shown, at various

expert core laboratory facilities at the University of Pittsburgh School of Medicine, also as shown. A total of 14 rats completed the protocol. Please see text for details.

(a) 2 Hours

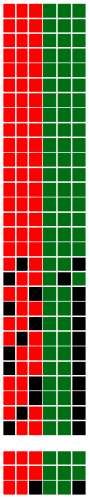

(b) 24 Hours

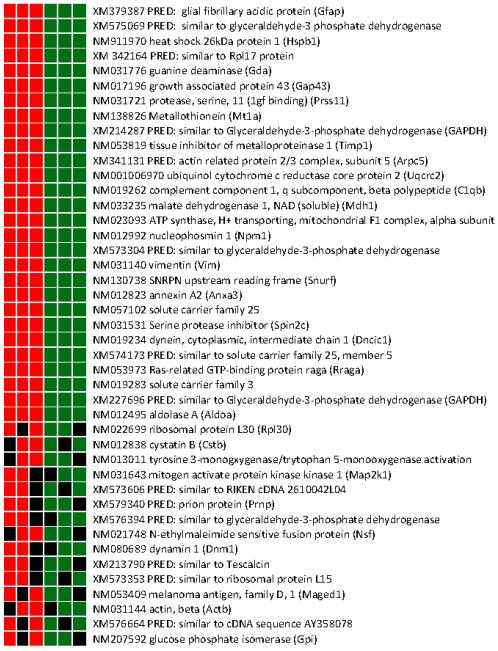

(c) 24 Hours Injured vs 2 Hours Injured

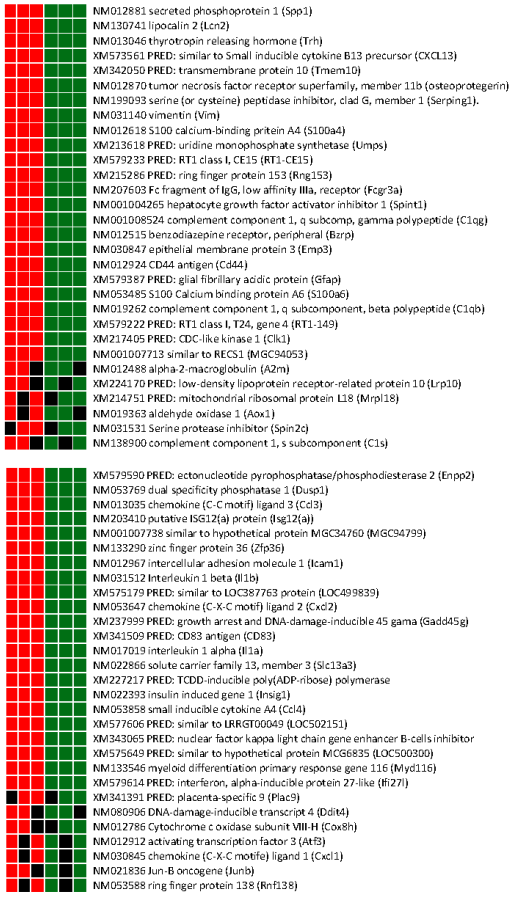

Figure 2. Expression grid pattern of differentially expressed genes in hippocampus comparing injured to sham rats at 2 h (a), 24 h (b), as well as injured rats at 24 h to injured rats at 2 h after blast injury (see methods for details). Predicted genes are labeled “PRED”, in which the mRNA sequence has been identified but the complete protein sequence is not verified. These genes were excluded from the analysis. When individual sample expression value is greater than 95 percentile compared to other group, it is represented as a red box. If less than 5 percentile, it is represented as a green box. If the expression value is within 5 and 95 percentile, it is represented as a black box. The associated tables (Tables 1-3) demonstrate the J5 values for each significant gene and its associated category.

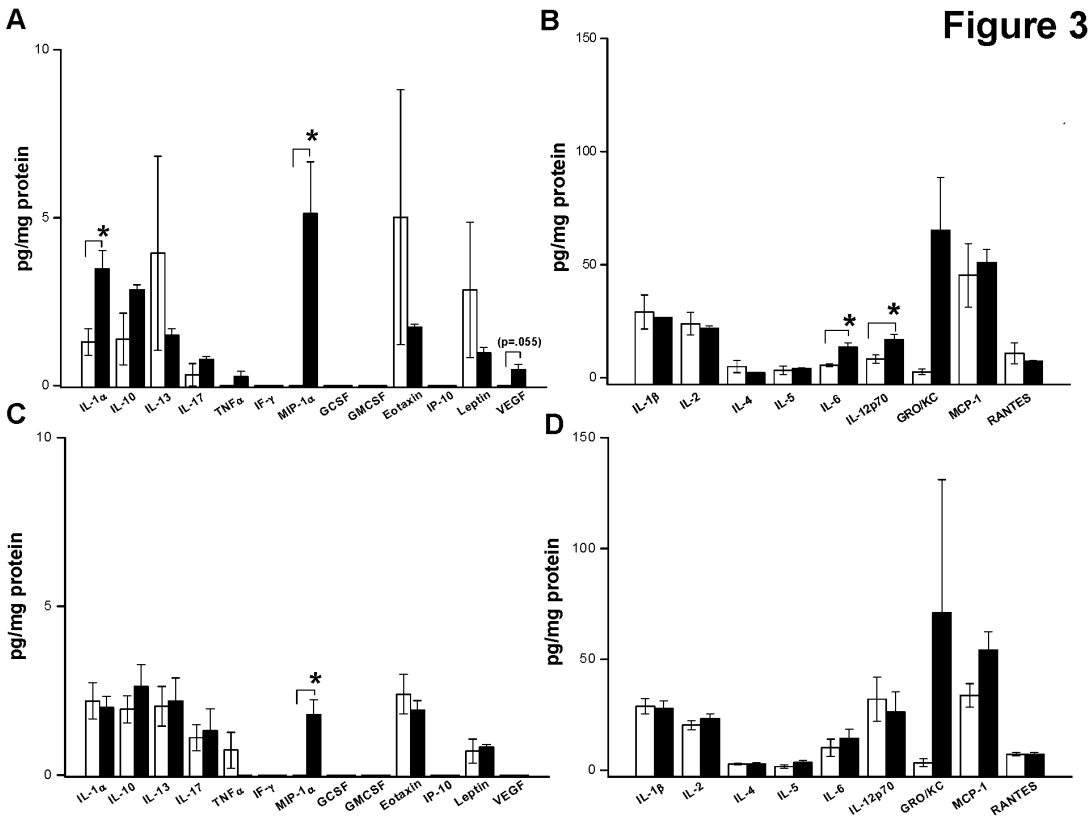

Figure 3A-D. Cytokine, chemokine, and growth factor protein levels after blast TBI or sham exposure. (A) Thirteen proteins with levels in the range of ~0-10 pg/mg protein at 2 h after injury are shown. Both the cytokine interleukin-1 alpha (IL-1α) and the chemokine macrophage inflammatory protein-1 alpha (MIP-1α) were increased vs. sham (**p*<0.05). The increase in MIP-1α was marked. A trend toward an increase in vascular endothelial growth factor (VEGF) was also seen, although it did not reach significance. (B) Nine proteins with levels in the range of ~10-100 pg/mg protein at 2 h after injury. Both IL-6 and IL-12p70 were increased vs. sham (**p*<0.05). The chemokine growth related oncogene KC (GRO/KC) showed a trend toward increase vs. sham. (C) Thirteen proteins with levels in the range of ~0-10 pg/mg protein at 24 h

after injury are shown. Only the chemokine macrophage inflammatory protein-1 alpha (MIP-1α) remained were increased vs. sham at 24 h (*P<0.05). (B) Nine proteins with levels in the range of ~10-100 pg/mg protein at 24 h after injury. A trend toward an increase in a second chemokine growth related oncogene KC (GRO/KC) was also seen although this did not reach significance. Data for IL-9 and IL-18 also did not differ between blast and sham groups at either 2 h or 24 h (data not shown). Please see text for details. Interleukin = IL, tumor necrosis factor alpha (TNFα), interferon gamma (IFNg), granulocyte colony stimulating factor (GCSF), granulocyte macrophage colony stimulating factor (GMCSF), monocyte chemotactic protein-1 (MCP-1), eotaxin, Interferon gamma-induced protein 10 (IP-10), regulated upon activation, normal T-cell (RANTES), leptin, and vascular endothelial growth factor (VEGF).

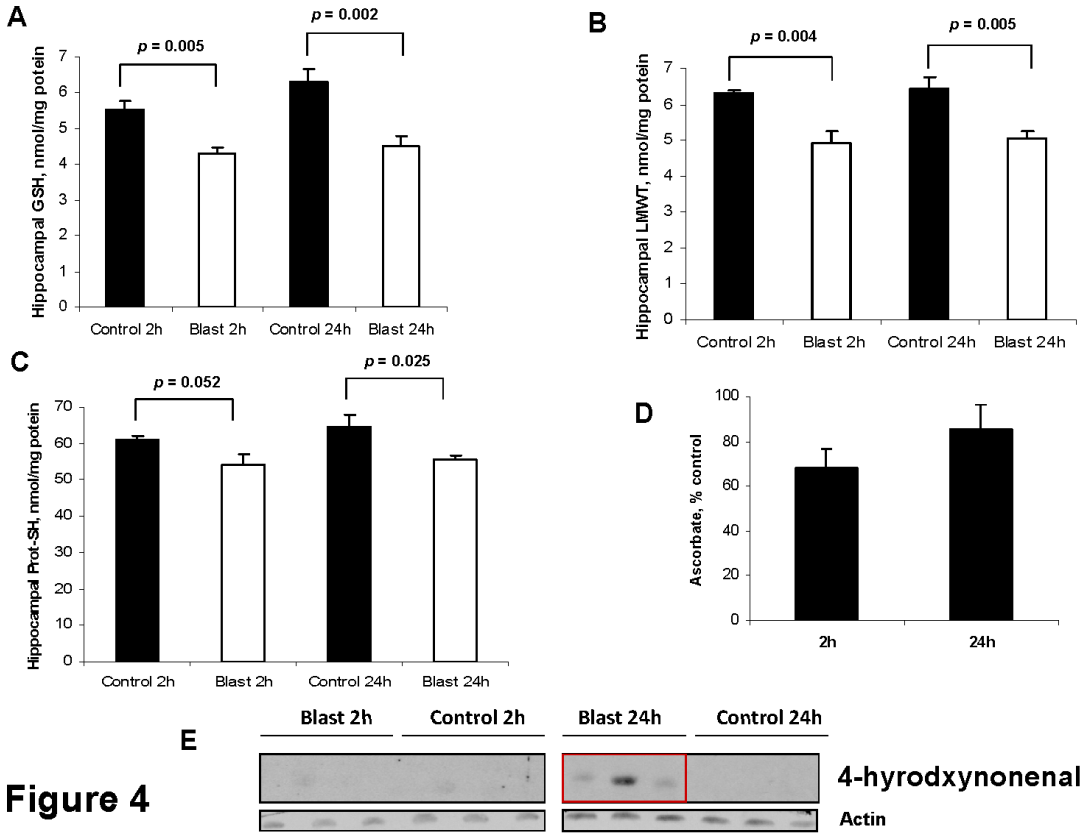

Figure 4

Figure 4A-E. Blast TBI induces oxidative stress in rat hippocampus at 2 h and 24 h after injury. (A) Blast TBI produced a significant decrease in reduced glutathione (GSH) in the hippocampus ipsilateral to the blast exposure at 2 h and 24 h after the insult (p = 0.005 and 0.002 vs. respective sham). (B) Low molecular weight thiols (LMWT) were also significantly reduced at both 2 and 24 h after blast injury (p = 0.004 and 0.005 vs. respective sham). (C) Protein thiols were also significantly reduced but only at 24 h after blast injury (p = 0.025 vs. respective sham), although a trend was seen at 2 h. (D) Ascorbate levels were not significantly decreased vs. respective sham, although a trend toward reduction (~30%) was seen at 2 h (p = 0.08). (E)

Screening for formation of 4-hydroxynoneanl adducts as evidence of lipid peroxidation on western blot revealed that they were present at 24 h but not 2 h after blast exposure.

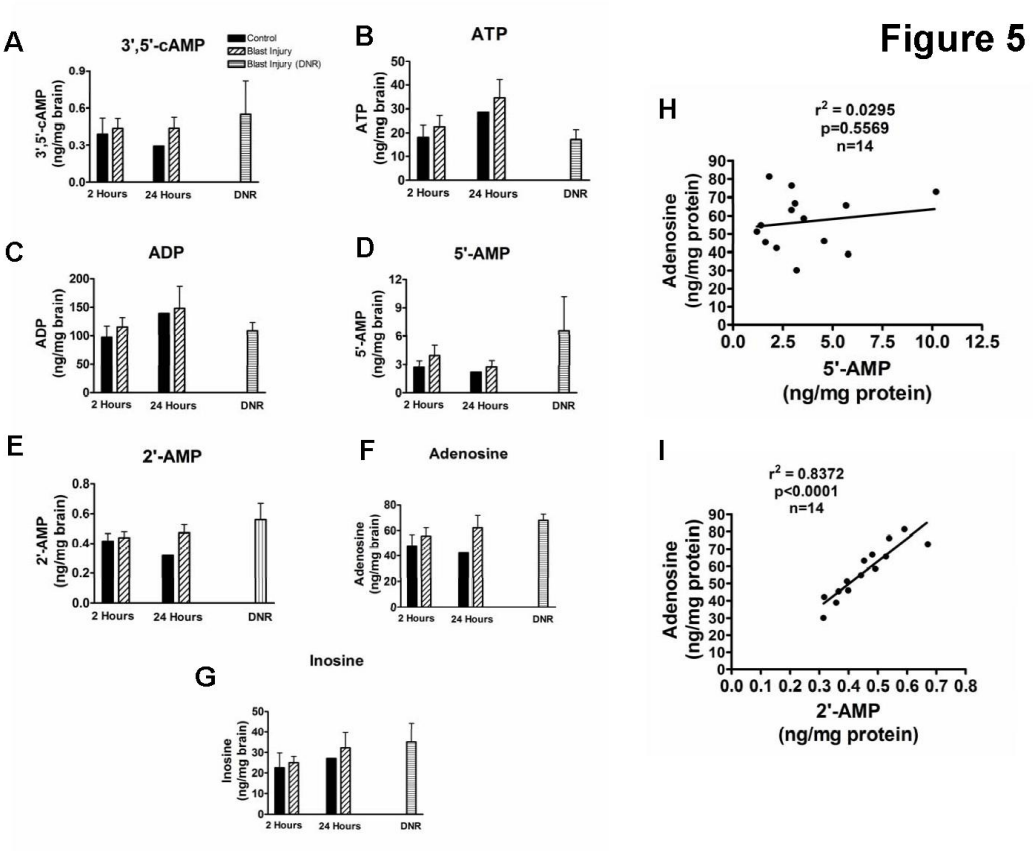

Figure 5A-I. Effect of blast TBI on purine metabolites in pre-frontal cortex at 2 h or 24 h after injury. LC-MS/MS assessment of (A) 3',5'-cAMP, (B) ATP, (C) ADP, (D) 5'-AMP, (E) 2'-AMP, (F) adenosine and (G) inosine using LC-MS/MS. There was no difference between sham and blast injury groups at either 2 h or 24 h after injury for any of these metabolites suggesting that energy failure and ATP depletion was not occurring. Levels of the endogenous neuroprotectant adenosine were not correlated with 5'-AMP (H), but were highly correlated 2'-AMP (I) suggesting the possibility that mRNA breakdown after blast TBI was leading to the generation of adenosine from 5'-AMP via the 2',3'-cAMP pathway, see text for details.

Journal of Neurotrauma

Table 1. Overexpressed (positive J5) and underexpressed (negative J5) genes in the ipsilateral hippocampus 2 h after blast exposure. Results are shown in order of decreasing J5 score

Gene Symbol	Gene Name	Accession	J5
Mt1a	Metallothionein	NM_138826.2	35.163
Hbb	Hemoglobin beta chain complex	NM_033234.1	28.035
Mt3	Metallothionein 3	NM_053968.2	26.539
4	65102_hemoglobin_alpha_adult_chain_1_(Hba-a1)	NM_013096.1	26.186
5	64138_synaptic_vesicle_glycoprotein_2b_(Sv2b)	NM_057207.2	25.773
6	53794_transthyretin_(Ttr)	NM_012681.1	-25.165
7	63461_PRED_similar_to_60S_ribosomal_protein_L37a_(LOC500547)	XM_575909.1	24.972
8	48559_PRED_ribosomal_protein_L37a_(pred)_(Rpl37a_pred)	XM_343587.1	24.033
9	56273_BCL2/adenovirus_E1B_19_kDa-interacting_protein_3_(Bnip3)	NM_053420.2	23.389
10	50959_cadherin_22_(Cdh22)	NM_019161.1	21.006
11	67501_PRED_ectonucleotide_pyrophosphatase/phosphodiesterase_2_(Enpp2)	XM_579590.1	-20.004
12	50318_ribosomal_protein_S15a_(Rps15a)	NM_053982.1	19.914
13	68233_dual_specificity_phosphatase_1_(Dusp1)	NM_053769.2	19.546
14	59917_PRED_cytochrome_c_oxidase_subunit_VIa_polypeptide_1_(Cox6a1)	XM_341094.2	19.433

15	59596_ATP_synthase_H+_transporting_mitochondrial_F0_complex_subunit_e_(Atp5i)	NM_080481.1	19.269
16	67909_Jun-B_oncogene_(Junb)	NM_021836.2	18.922
17	57918_PRED_similar_to_Finkel-Biskis-Reilly_murine_sarcoma_virus_(FBR-MuSV)_ubiquitously_expressed_(fox_derived)_(LOC499305)	XM_574605.1	18.855
18	52798_PRED_Finkel-Biskis-Reilly_murine_sarcoma_virusubiquitously_expressed_(Fau)	XM_342000.2	18.422
19	56492_PRED_similar_to_ribosomal_protein_S26_(LOC298785)	XM_213058.2	18.041
20	60481_PRED_similar_to_60S_ribosomal_protein_L32_(LOC302445)	XM_213183.2	17.705
21	63177_insulin-like_growth_factor_2_(Igf2)	NM_031511.1	-17.689
22	53083_PRED_similar_to_novel_cell_death-regulatory_protein_GRIM19_(LOC290671)	XM_214305.3	17.668
23	62109_ribosomal_protein_S14_(Rps14)	NM_022672.1	17.463
24	69225_cholecystokinin_(Cck)	NM_012829.1	17.254
25	60479_PRED_similar_to_60S_ribosomal_protein_L37a_(LOC302528)	XM_228717.1	17.23
26	57073_proteolipid_protein_(Plp)	NM_030990.1	-17.12
27	70009_PRED_ribosomal_protein_L27a_(pred)_(Rpl27a_pred)	XM_215041.3	17.094
28	57081_ribosomal_protein_S21_(Rps21)	NM_031111.1	17.077
29	49934_PRED_nuclear_factor_of_kappa_light_chain_gene_enhancer_in_B-cells_inhibitor_alpha_(Nfkbia)	XM_343065.2	17.074
30	52466_PRED_ribosomal_protein_s25_(Rps25)	XM_579143.1	16.851

31	50109_PRED_similar_to_ribosomal_protein_L31_(LOC299935)	XM_213094.2	16.849
32	48223_PRED_similar_to_ribosomal_protein_S23_(LOC498360)	XM_573594.1	16.749
33	49821_ribosomal_protein_L32_(Rpl32)	NM_013226.1	16.667
34	60315_diazepam_binding_inhibitor_(Dbi)	NM_031853.3	16.525
35	65774_PRED_similar_to_ribosomal_protein_S19_(LOC503110)	XM_578630.1	16.385
36	49079_ribosomal_protein_L41_(Rpl41)	NM_139083.1	16.335
37	48590_ribosomal_protein_S10_(Rps10)	NM_031109.1	16.287
38	49912_PRED_similar_to_ribosomal_protein_S12_(LOC309408)	XM_219903.2	16.107
39	65073_PRED_Transferrin_(Tf)	XM_579389.1	-16.056
40	70369_PRED_similar_to_RIKEN_cDNA_3110001N18_(LOC366188)	XM_345431.1	15.984
41	62237_PRED_ubiquinol-cytochrome_c_reductase_binding_protein_(pred)_(Uqcrb_pred)	XM_343225.2	15.914
42	52471_protease_serine_23_(Prss23)	NM_001007691.1	-15.899
43	63466_ribosomal_protein_L29_(Rpl29)	NM_017150.1	15.813
44	56800_NADH_dehydrogenase_(ubiquinone)_1_alpha_subcomplex_11_(Ndufa11)	NM_212517.1	15.787
	65114_ubiquinol-cytochrome_c_reductase_hinge_protein_(Uqcrh)	NM_001009480.1	15.742
46	48172_ribosomal_protein_L35_(Rpl35)	NM_212511.1	15.702
47	63159_PRED_similar_to_ribosomal_protein_L34_(LOC307135)	XM_225596.1	15.569

48	50133_ribosomal_protein_S26_(Rps26)	NM_013224.1	15.53
49	58168_cytochrome_c_oxidase_subunit_VIIb_(Cox7b)	NM_182819.1	15.51
50	50093_PRED_NADH_dehydrogenase_(ubiquinone)_1_beta_subcomplex_2_(pred)_(Ndufb2_pred)	XM_342664.2	15.415
51	57561_PRED_similar_to_40S_ribosomal_protein_S19_(LOC502302)	XM_218303.1	15.264

Table 2. Overexpressed (positive J5) and underexpressed (negative J5) genes in the ipsilateral hippocampus 24 h after blast exposure. Shown in order of decreasing J5 score

Rank	Name	J5	ACC_NO
1	68224_PRED_glial_fibrillary_acidic_protein_(Gfap)	238.816	XM_579387.1
2	64138_synaptic_vesicle_glycoprotein_2b_(Sv2b)	-178.53	NM_057207.2
3	66032_PRED_similar_to_glyceraldehyde-3-phosphate_dehydrogenase_(LOC500506)	104.238	XM_575868.1
4	65073_PRED_Transferrin_(Tf)	-93.134	XM_579389.1
5	59800_PRED_similar_to_ORF4_(LOC361942)	-76.364	XM_342241.2
6	53757_PRED_similar_to_Tubulin_alpha-2_chain_(Alpha-tubulin_2)_(LOC500929)	-74.248	XM_576339.1
7	64101_PRED_hypothetical_gene_supported_by_BC087105_(LOC500856)	-72.23	XM_580130.1
8	66108_PRED_3-hydroxy-3-methylglutaryl-Coenzyme_A_synthase_1_(Hmgcs1)	-70.16	XM_579405.1
9	70349_heat_shock_27kDa_protein_1_(Hspb1)	69.913	NM_031970.1
10	53820_PRED_similar_to_Rpl17_protein_(LOC361869)	67.616	XM_342164.2
11	67056_PRED_similar_to_testin_(LOC503278)	66.574	XM_578812.1
12	56963_PRED_similar_to_ORF4_(LOC498048)	-65.987	XM_573248.1
13	60315_diazepam_binding_inhibitor_(Dbi)	-65.766	NM_031853.3
14	58313_PRED_similar_to_glyceraldehyde-3-phosphate_dehydrogenase_(LOC500983)	64.087	XM_576394.1
15	67501_PRED_ectonucleotide_pyrophosphatase/phosphodiesterase_2_(Enpp2)	-63.742	XM_579590.1
16	68346_tubulin_alpha_1_(Tuba1)	-63.423	NM_022298.1
17	56273_BCL2/adenovirus_E1B_19_kDa-interacting_protein_3_(Bnip3)	-63.352	NM_053420.2
18	53205_PRED_similar_to_60S_ribosomal_protein_L17_(L23)_(Amino_acid_starvation-induced_protein)_(ASI)_(LOC367398)	-61.607	XM_576661.1
19	65816_guanine_deaminase_(Gda)	61.181	NM_031776.1
20	66022_PRED_plakophilin_4_(pred)_(Pkp4_pred)	-60.531	XM_215733.3
21	50398_PRED_similar_to_RIKEN_cDNA_2410116I05_(LOC363377)	-59.531	XM_343712.2
22	60643_serum/glucocorticoid_regulated_kinase_(Sgk)	57.752	NM_019232.1
23	65851_PRED_similar_to_LRRG00116_(LOC362543)	-57.401	XM_342864.2

24	64861_cyclic_nucleotide_phosphodiesterase_1_(Cnp1)	-56.878	NM_012809.1
25	66358_actin_beta_(Actb)	55.115	NM_031144.2
26	64690_growth_associated_protein_43_(Gap43)	55.06	NM_017195.1
27	64865_ribosomal_protein_L17_(Rpl17)	-54.338	NM_201415.1
28	64748_N-myc_downstream_regulated_gene_2_(Ndrg2)	-53.958	NM_133583.1
29	57328_PRED_similar_to_Ac1262_(LOC363492)	-53.4	XM_343815.2
30	67903_carbonic_anhydrase_2_(Ca2)	-53.371	NM_019291.1
31	57073_proteolipid_protein_(Plp)	-50.942	NM_030990.1
32	64064_protease_serine_11_(Igf_binding)_(Prss11)	49.761	NM_031721.1
33	53575_Metallothionein_(Mt1a)	48.76	NM_138826.2
34	66191_ribonuclease_RNase_A_family_4_(Rnase4)	-47.407	NM_020082.2
35	65814_myelin_and_lymphocyte_protein_(Mal)	-47.3	NM_012798.1
36	60399_selenoprotein_W_muscle_1_(Sepw1)	-46.179	NM_013027.1
37	53801_ATPase_H+_transporting_V0_subunit_C_(Atp6v0c)	-46.147	NM_130823.2
38	57715_PRED_similar_to_LRRG00135_(LOC501637)	-45.936	XM_577034.1
39	51075_PRED_nel-like_2_homolog_(chicken)_(Nell2)	45.847	XM_579504.1
40	58188_glycoprotein_38_(Gp38)	45.463	NM_019358.1
41	51219_metallothionein_3_(Mt3)	-44.751	NM_053968.2
42	56089_N-ethylmaleimide_sensitive_fusion_protein_(Nsf)	44.528	NM_021748.1
43	70319_PRED_Jun_D_proto-oncogene_(Jund)	-44.094	XM_579658.1
44	69046_myelin_oligodendrocyte_glycoprotein_(Mog)	-43.883	NM_022668.1
45	50141_calcium/calmodulin-dependent_protein_kinase_II_inhibitor_1_(Camk2n1)	-43.749	NM_173337.1
46	63461_PRED_similar_to_60S_ribosomal_protein_L37a_(LOC500547)	-43.535	XM_575909.1
47	67911_calreticulin_(Calr)	-42.917	NM_022399.1
48	52581_protein_phosphatase_3_catalytic_subunit_alpha_isoform_(Ppp3ca)	-42.451	NM_017041.1
49	64945_reticulon_4_(Rtn4)	-42.348	NM_031831.1
50	60797_PRED_similar_to_Ac1147_(LOC310926)	41.71	XM_227769.2
51	61449_PRED_similar_to_Glyceraldehyde-3-phosphate_dehydrogenase_(GAPDH)_(LOC290634)	41.416	XM_214287.3
52	65242_PRED_calmodulin_1_(Calm1)	-41.244	XM_579543.1
53	57628_ARP2_actin-related_protein_2_homolog_(yeast)_(Actr2)	-40.818	NM_001009268.1

54	55545_tyrosine_3-monooxygenase/tryptophan_5-monooxygenase_activation_protein_zeta_polypeptide_(Ywhaz)	40.56	NM_013011.1
55	55306_PRED_similar_to_RIKEN_cDNA_2610042L04_(LOC498371)	39.677	XM_573606.1
56	52278_PRED_prion_protein_(Prnp)	38.656	XM_579340.1
57	54246_ATPase_Na+/K+_transporting_alpha_2_polypeptide_(Atp1a2)	-38.12	NM_012505.1
58	47800_fatty_acid_binding_protein_7_brain_(Fabp7)	-38.103	NM_030832.1
59	62559_tissue_inhibitor_of_metalloproteinase_1_(Timp1)	37.855	NM_053819.1
60	56078_tumor_protein_translationally-controlled_1_(Tpt1)	-37.607	NM_053867.1
61	50209_PRED_actin_related_protein_2/3_complex_subunit_5_(pred)_(Arpc5_pred)	37.341	XM_341131.2
62	48559_PRED_ribosomal_protein_L37a_(pred)_(Rpl37a_pred)	-37.317	XM_343587.1
63	65995_ATPase_H+_transporting_V1_subunit_B_isoform_2_(Atp6v1b2)	37.104	NM_057213.2
64	54015_PRED_similar_to_L-lactate_dehydrogenase_A_chain_(LDH-A)_(LDH_muscle_subunit)_(LDH-M)_(LOC500965)	37.018	XM_576374.1
65	52257_stearoyl-Coenzyme_A_desaturase_2_(Scd2)	-36.929	NM_031841.1
66	67309_PRED_similar_to_Retrovirus-related_POL_polyprotein_(LOC362315)	-36.921	XM_342631.2
67	66374_LIM_domain_only_4_(Lmo4)	-36.828	NM_001009708.1
68	58863_PRED_similar_to_Tescalcin_(LOC288689)	35.721	XM_213790.3
69	47777_PRED_similar_to_LRRG00135_(LOC501548)	-34.265	XM_576950.1
70	64580_protein_phosphatase_3_regulatory_subunit_B_alpha_isoform_(calcineurin_B_type_I)_(Ppp3r1)	-33.858	NM_017309.2
71	67723_tubulin_beta_2_(Tubb2)	-33.638	NM_199094.1
72	54363_PRED_LOC500721_(LOC500721)	-33.432	XM_580114.1
73	57098_lysosomal-associated_protein_transmembrane_4A_(Laptm4a)	-33.427	NM_199384.1
74	48846_myelin_basic_protein_(Mbp)	-33.262	NM_017026.1
75	48072_phosphatidylethanolamine_binding_protein_(Pbp)	33.202	NM_017236.1
76	63688_ubiquinol_cytochrome_c_reductase_core_protein_2_(Uqcrc2)	33.148	NM_001006970.1
77	55248_ribosomal_protein_L30_(Rpl30)	32.804	NM_022699.2
78	60306_chondroitin_sulfate_proteoglycan_5_(Cspg5)_transcript_variant_1	-32.792	NM_019284.1
79	61448_complement_component_1_q_subcomponent_beta_polypeptide_(C1qb)	32.534	NM_019262.1
80	55787_PRED_similar_to_RIKEN_cDNA_4930555G01_(LOC498375)	32.514	XM_573610.1
81	68428_fasciculation_and_elongation_protein_zeta_1_(zygin_I)_(Fez1)	-32.454	NM_031066.1
82	61404_cystatin_C_(Cst3)	-32.403	NM_012837.1
83	59957_calcium/calmodulin-dependent_protein_kinase_II_beta_subunit_(Camk2b)	-32.239	NM_021739.1

84	55606_malate_dehydrogenase_1_NAD_(soluble)_(Mdh1)	32.113	NM_033235.1
85	54601_neurogranin_(Nrgn)	-32.094	NM_024140.2
86	50017_PRED_similar_to_Small_membrane_protein_1_(pred)_(LOC298552)	-31.812	XM_216545.3
87	53344_ATP_synthase_H+_transporting_mitochondrial_F1_complex_alpha_subunit_isoform_1_(Atp5a1)	31.591	NM_023093.1
88	69434_similar_to_Nur77_downstream_protein_2_(MGC105647)	-31.347	NM_001007008.1
89	61545_chemokine_(C-X3-C_motif)_ligand_1_(Cx3cl1)	-31.229	NM_134455.1
90	59239_PRED_similar_to_T-complex_associated-testis-expressed_1-like_(Protein_91/23)_(LOC501521)	-31.201	XM_576923.1
91	64944_nucleophosmin_1_(Npm1)	30.119	NM_012992.2
92	66984_PRED_similar_to_glyceraldehyde-3-phosphate_dehydrogenase_(LOC498099)	29.995	XM_573304.1
93	62489_PRED_histone_deacetylase_11_(pred)_(Hdac11_pred)	-29.814	XM_238362.3
94	53421_aldolase_C_fructose-biphosphate_(Aldoc)	-29.776	NM_012497.1
95	67589_PRED_similar_to_LRRG00116_(LOC500867)	-29.478	XM_576265.1
96	52641_PRED_similar_to_Eph_receptor_A4_(LOC316539)	-29.462	XM_244186.3
97	55111_PRED_polyubiquitin_(Ubb)	-28.934	XM_579661.1
98	54242_vimentin_(Vim)	28.92	NM_031140.1
99	60033_tetraspan_2_(Tspan2)	-28.641	NM_022589.1
100	52135_PRED_nucleoside_phosphorylase_(Np)	-28.542	XM_214155.3
101	63348_ATPase_Ca++_transporting_cardiac_muscle_slow_twitch_2_(Atp2a2)	-28.174	NM_017290.1
102	50549_PRED_similar_to_ribosomal_protein_L15_(LOC498143)	28.158	XM_573353.1
103	57629_SNRPN_upstream_reading_frame_(Snurf)	28.101	NM_130738.1
104	53861_PRED_cyclin_I_(pred)_(Ccni_pred)	-28.1	XM_214007.3
105	54685_asparaginase-like_sperm_autoantigen_(Asrgl1)	-28.073	NM_145089.2
106	57519_annexin_A3_(Anxa3)	27.934	NM_012823.1
107	55334_ribosomal_protein_L9_(Rpl9)	-27.874	NM_001007598.2
108	63257_cystatin_B_(Cstb)	27.841	NM_012838.1
109	63580_lysosomal_membrane_glycoprotein_1_(Lamp1)	-27.467	NM_012857.1
110	56027_heat_shock_70kD_protein_5_(Hspa5)	-27.204	NM_013083.1
111	56464_Sec11-like_3_(S_cerevisiae)_(Sec11l3)	-27.158	NM_153628.1
112	48685_solute_carrier_family_25_(mitochondrial_carrier;_adenine_nucleotide_translocator)_member_5_(Slc25a5)	26.761	NM_057102.1
113	66571_clusterin_(Clu)	26.725	NM_053021.2

114	50412_beta-2_microglobulin_(B2m)	26.336	NM_012512.1
115	59171_mitogen_activated_protein_kinase_kinase_1_(Map2k1)	26.192	NM_031643.3
116	48424_putative_ISG12(a)_protein_(isg12(a))	-26.13	NM_203410.1
117	61561_ferritin_heavy_polypeptide_1_(Fth1)	-26.123	NM_012848.1
118	60484_Serine_protease_inhibitor_(Spin2c)	25.975	NM_031531.1
119	52089_PRED_similar_to_ribosomal_protein_L21_(LOC293642)	-25.798	XM_212883.3
120	60218_dynein_cytoplasmic_intermediate_chain_1_(Dncic1)	25.396	NM_019234.1
121	52149_PRED_similar_to_solute_carrier_family_25_member_5_(LOC498885)	25.28	XM_574173.1
122	60826_PRED_similar_to_Glycolipid_transfer_protein_(LOC288707)	-25.017	XM_213793.3
123	54968_crystallin_alpha_B_(Cryab)	24.924	NM_012935.2
124	58278_calmodulin_2_(Calm2)	-24.813	NM_017326.1
125	48422_Ras-related_GTP-binding_protein_ragA_(Rraga)	24.729	NM_053973.1
126	62993_peroxiredoxin_6_(Prdx6)	-24.669	NM_053576.1
127	66828_pregnancy_upregulated_non-ubiquitously_expressed_CaM_kinase_(Pnck)	24.604	NM_017275.1
128	69562_dynamin_1_(Dnm1)	24.573	NM_080689.2
129	59917_PRED_cytochrome_c_oxidase_subunit_VIa_polypeptide_1_(Cox6a1)	-24.313	XM_341094.2
130	69749_solute_carrier_family_3_(activators_of_dibasic_and_neutral_amino_acid_transport)_member_2_(Slc3a2)	24.305	NM_019283.1
131	65297_neurofilament_light_polypeptide_(Nfl)	23.585	NM_031783.1
132	51621_PRED_similar_to_Glyceraldehyde-3-phosphate_dehydrogenase_(GAPDH)_(LOC295452)	23.542	XM_227696.3
133	69972_SPARC-like_1_(mast9_hevin)_(Sparcl1)	-23.518	NM_012946.1
134	69307_melanoma_antigen_family_D_1_(Maged1)	23.505	NM_053409.1
135	53094_G_protein-coupled_receptor_56_(Gpr56)	-23.49	NM_152242.1
136	67819_aldolase_A_(Aldoa)	23.179	NM_012495.1
137	52165_integral_membrane_protein_2B_(Itm2b)	22.974	NM_001006963.1
138	53919_PRED_similar_to_cDNA_sequence_AY358078_(LOC501245)	22.889	XM_576664.1
139	49011_macrophage_migration_inhibitory_factor_(Mif)	-22.813	NM_031051.1
140	63888_glucose_phosphate_isomerase_(Gpi)	22.548	NM_207592.1
141	68784_thyrotropin_releasing_hormone_(Trh)	22.292	NM_013046.2
142	48590_ribosomal_protein_S10_(Rps10)	-22.227	NM_031109.1

Table 3. Impact Analysis: Ipsilateral hippocampus 2 h after blast exposure

Rank	Pathway name	Impact factor	# Genes in pathway	# Input genes in pathway	# Pathway genes on array	% Input genes in pathway	% Pathway genes in input	p-value
1	Ribosome	30.538	77	9	58	31.034	11.688	1.27E-13
2	Cardiac muscle contraction	5.23	81	2	49	6.897	2.469	0.01175
3	Parkinson's disease	4.813	157	2	61	6.897	1.274	0.017834
4	Huntington's disease	4.05	213	2	92	6.897	0.939	0.038257
5	Alzheimer's disease	3.828	213	2	104	6.897	0.939	0.047754

Table 4. Impact Analysis: Ipsilateral hippocampus 24 h after blast exposure

Rank	Pathway name	Impact factor	# Genes in pathway	# Input genes in pathway	# Pathway genes on array	% Input genes in pathway	% Pathway genes in input	p-value
2	Alzheimer's disease	11.7	213	8	104	8	3.756	2.63E-05
3	Long-term potentiation	10.733	71	5	52	5	7.042	3.27E-04
4	Calcium signaling pathway	9.011	189	7	131	7	3.704	8.10E-04
5	VEGF signaling pathway	7.828	69	4	48	4	5.797	0.002279
7	Cardiac muscle contraction	7.163	81	4	49	4	4.938	0.00246
8	Ribosome	6.264	77	4	58	4	5.195	0.004548
9	Parkinson's disease	6.123	157	4	61	4	2.548	0.005447
11	Antigen processing and presentation	5.608	100	3	36	3	3	0.008293
10	Glioma	5.864	64	3	40	3	4.688	0.011098
13	Protein export	5.141	12	1	1	1	8.333	0.011651
20	Amyotrophic lateral sclerosis (ALS)	4.744	65	3	50	3	4.615	0.020255
22	Huntington''s disease	4.548	213	4	92	4	1.878	0.02221
16	PPAR signaling pathway	4.987	70	3	52	3	4.286	0.022462
19	Melanogenesis	4.814	96	3	54	3	3.125	0.024796
17	Gap junction	4.821	90	3	57	3	3.333	0.028532
14	Natural killer cell mediated cytotoxicity	5.029	98	3	62	3	3.061	0.035385
25	GnRH signaling pathway	4.366	91	3	62	3	3.297	0.035385
15	Axon guidance	5.019	123	3	66	3	2.439	0.041425
21	T cell receptor signaling pathway	4.626	110	3	71	3	2.727	0.049655
24	Wnt signaling pathway	4.368	142	3	77	3	2.113	0.060501
23	B cell receptor signaling pathway	4.477	67	2	40	2	2.985	0.078789
27	MAPK signaling pathway	3.973	253	4	170	4	1.581	0.136474

31	Apoptosis	3.346	87	2	59	2	2.299	0.150408
32	ErbB signaling pathway	2.858	83	2	60	2	2.41	0.154472
33	Biosynthesis of unsaturated fatty acids	2.596	26	1	18	1	3.846	0.190354
34	Thyroid cancer	2.561	29	1	20	1	3.448	0.209151
38	Bladder cancer	2.366	36	1	25	1	2.778	0.254274
37	Insulin signaling pathway	2.393	130	2	87	2	1.538	0.269282

TABLES